

図3 scFvを利用したATLがん幹細胞特異的miRNAデリバリー概念図  
図に示すように、がん幹細胞の表面マーカーの同定をもとにしてその単クローン抗体を利用してscFvを作成し、それをmiRNAデリバリーの担体として利用することを目指す。

ラフィー精製，サイズ排除カラムクロマトグラフィーにより最終精製を行った。可溶性画分からの最終精製でモノマー体での精製が困難であったものは，変性剤(グアニジン塩酸塩)を用いて可溶化し，Niアフィニティーカラムクロマトグラフィー精製，巻き戻し操作を経て，サイズ排除カラムクロマトグラフィーにより最終精製を行った。抗原も同様に発現確認を行い，可溶性画分での精製が可能であったため，上記の方法で最終精製を行った。

#### 4. 融合単鎖抗体の物性機能解析

得られたscFvの抗体機能を確認するために，表面プラズモン共鳴SPR(surface plasmon resonance)と等温滴定型カロリメーター(isothermal titration calorimetry, ITC)を用いて抗原との結合解析を行った。これまでに，われわれが設計したscFvの大量精製は成功し，SPRおよびITCを用いた抗原結合解析の結果，ポジティブコントロールのIgGが非常に強力な親和性と遅い解離速度を有していることが確認され，同様にscFvとペプチド融合scFvも抗体の特性である高い親和性と遅い解離速度を有していることが確認された。しかし，miRNAとの結合のために付加したカチオン性ペプチドは，大腸菌由来のDNAやRNAと結合し，カチオン性ペプチド-ヒスチジンタグまでの荷電残基に核酸が大量に存在していることが明らかになり，精製法の工夫および実験計画の改善が進められている。現在，これらの成果と経験に基づき，scFv結合miR-

31の生物学的効果を検証する実験を開始している(未発表)。

#### おわりに

本稿では，ATL細胞がNF-κBの恒常的活性化を示し，増殖と細胞死耐性に必須の分子機構となっていることを前提に，筆者らが取り組んでいる新規治療法開発研究の現状を可能な範囲で紹介した。ATL「がん幹細胞」の探索と細胞特性の解析にdrug delivery systemとしてのscFvの活用をリンクさせて，新規の治療法の開発を目指すのが研究の課題である。進捗に伴い，さまざまな課題が浮かび上がってきたが，それらの課題を近々に乗り越えることを目指して努力中である。

#### 文献

- 1) Yamagishi M, Watanabe T. Molecular hallmarks of adult T cell leukemia. *Front Microbiol* 2012; 3: 334.
- 2) Mori N, Fujii M, Ikeda S, et al. Constitutive activation of NF-κB in primary adult T-cell leukemia cells. *Blood* 1999; 93: 2360.
- 3) Yamagishi M, Watanabe T. New paradigm of T cell signaling: learning from malignancies [review]. *J Clin Cell Immunol* 2012; S12: 007.
- 4) Inoue J, Gohda J, Akiyama T, Semba K. NF-kappaB activation in development and progression of cancer. *Cancer Sci* 2007; 98: 268.

- 5) Shackleton M, Quintana E, Fearon ER, Morrison SJ. Heterogeneity in cancer : cancer stem cells versus clonal evolution. *Cell* 2009 ; 138 : 822.
- 6) Yamagishi M, Nakano K, Miyake A, et al. Polycomb-mediated loss of miR-31 activates NIK-dependent NF- $\kappa$ B pathway in adult T cell leukemia and other cancers. *Cancer Cell* 2012 ; 21 : 121.
- 7) Mori N, Fujii M, Ikeda S, et al. Constitutive activation of NF- $\kappa$ B in primary adult T-cell leukemia cells. *Blood* 1999 ; 93 : 2360.
- 8) Hironaka N, Mochida K, Mori N, et al. Tax-Independent Constitutive I $\kappa$ B kinase activation in adult T-cell leukemia cells. *Neoplasia* 2004 ; 6 : 266.
- 9) Watanabe M, Ohsugi T, Shoda M, et al. Dual targeting of transformed and untransformed HTLV-1-infected T cells by DHMEQ, a potent and selective inhibitor of NF- $\kappa$ B, as a strategy for chemoprevention and therapy of adult T-cell leukemia. *Blood* 2005 ; 106 : 2462.
- 10) Saitoh Y, Yamamoto N, Dewan MZ, et al. Over-expressed NF- $\kappa$ B-inducing kinase contributes to the tumorigenesis of adult T-cell leukemia and Hodgkin Reed-Sternberg cells. *Blood* 2008 ; 111 : 5118.
- 11) Dewan MZ, Terashima K, Taruishi M, et al. Rapid tumor formation of human T-cell leukemia virus type 1-infected cell lines in novel NOD-SCID/ $\gamma$ mac(null) mice : suppression by an inhibitor against NF- $\kappa$ B. *J Virol* 2003 ; 77 : 5286.
- 12) Lapidot T, Sirard C, Vormoor J, et al. A cell initiating human acute myeloid leukaemia after transplantation into SCID mice. *Nature* 1994 ; 367 : 645.
- 13) Yamazaki J, Mizukami T, Takizawa K, et al. Identification of cancer stem cells in a Tax-transgenic (Tax-Tg) mouse model of adult T-cell leukemia/lymphoma. *Blood* 2009 ; 114 : 2709.
- 14) 厚生労働科学研究費補助金 第3次対がん総合戦略研究事業. 成人T細胞白血病のがん幹細胞の同定とそれを標的とした革新的予防・診断・治療法の確立(研究代表者・渡邊俊樹)(H21-3次がん一般-002). 平成23年度総合研究報告書.

\*            \*            \*

## 特集

## 血液疾患におけるエピゲノム異常と治療

ATL発症における  
エピゲノム解析の進歩\*山岸 誠\*\*  
渡邊 俊樹\*\*

**Key Words** : adult T cell leukemia/lymphoma (ATL), human T cell leukemia virus type 1 (HTLV-1), DNA methylation, Polycomb, miRNA

## はじめに

成人 T 細胞白血病 (adult T cell leukemia/lymphoma ; ATL) はヒト T 細胞白血病ウイルス I 型 (human T cell leukemia virus type 1 ; HTLV-1) の感染によって引き起こされる重篤な T 細胞性白血病/リンパ腫である。50~60年という長い潜伏期間に HTLV-1 感染 T 細胞に複数の遺伝子異常が蓄積し、きわめて予後不良な ATL を発症する<sup>1)</sup>。

これまでの多くの研究から、HTLV-1 がコードするウイルス遺伝子、特に Tax と HBZ による病原性については非常に多くの研究がされており、HTLV-1 の感染が ATL の分子レベルの背景となっていることは明白である<sup>2)</sup>。しかし一方で、実際の ATL 細胞では HBZ を除くウイルス遺伝子の発現は稀であり、感染後期に起こる腫瘍細胞の形成、維持、悪性化、薬剤耐性などの分子メカニズムに関する研究はいまだ発展途上である<sup>3)</sup>。

ATL が発見された当初から染色体異常の研究が行われ、HTLV-1 感染細胞の終末像である ATL 細胞にはゲノム異常が蓄積しているという事実が

ある。初期の染色体解析の結果では 96% の症例で染色体異常があり、ATL の背景にゲノム異常の蓄積が存在するのは確かである。しかし他の悪性リンパ腫やがんと比較すると、ATL には腫瘍細胞を特徴づけるような定義的な染色体転座や変異はなく、ゲノムの異常はむしろ多様性があるといえる<sup>3)</sup>。

われわれは最近、多数の臨床検体を用いた遺伝子発現の大規模解析の結果から、ATL 細胞は非常に均一で異常な遺伝子発現パターンを持つ集団であることを明らかにした<sup>4)</sup>。さらに、ATL 細胞には特徴的なシグナル伝達系の異常があり、腫瘍細胞の生存や増殖の基軸となっているが、その背景にはエピジェネティックな異常の蓄積があることが明らかとなってきた。つまり ATL 細胞は多様なゲノムおよびエピゲノムの異常を背景に、さらに複数個のイベントが ATL 細胞の特徴的な遺伝子発現を支配していると考えられる (図 1)<sup>4)5)</sup>。

ATL におけるエピゲノム解析は、DNA、ヒストン修飾のどちらも網羅的な解析は完了しておらず、全体像がつかめているとは言い難い。しかし、発現パターンに基づいた各遺伝子の制御機構の解析が精力的に進められており、またエピジェネティック阻害剤を用いた研究成果からも、ATL 細胞の背景にエピゲノム異常の蓄積があ

\* The state of the art in epigenomics of adult T cell leukemia.

\*\* Makoto YAMAGISHI, Ph.D. & Toshiki WATANABE, M.D., Ph.D.: 東京大学大学院新領域創成科学研究科メディカルゲノム専攻病態医療科学分野 [〒108-8639 東京都港区白金台4-6-1] ; Laboratory of Tumor Cell Biology, Department of Medical Genome Sciences, Graduate School of Frontier Sciences, The University of Tokyo, Tokyo 108-8639, JAPAN

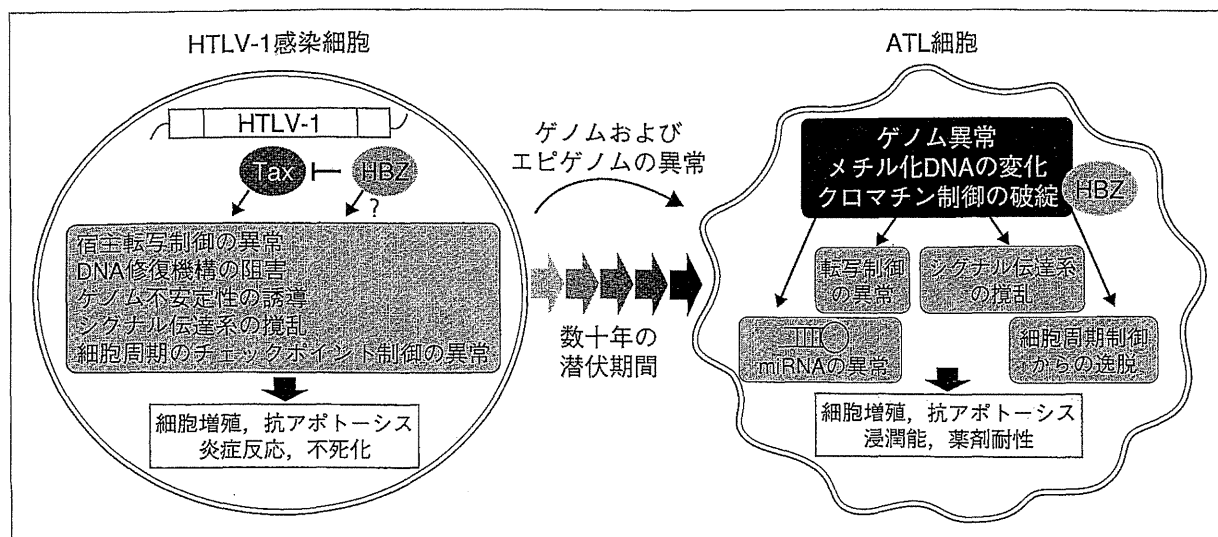


図1 HTLV-1感染細胞からATL細胞へ

HTLV-1感染初期にはウイルス遺伝子による分子レベルでのさまざまな攪乱が起こる。長期の潜伏期間を経て増殖したATL細胞ではゲノムおよびエピゲノムの異常を背景に、アポトーシス抵抗性、NF- $\kappa$ B経路の活性化、miRNAの発現低下など、特徴的な分子異常を示す。

ることは確からしい。本稿では各研究成果を紹介しながらATLにおけるエピジェネティック異常の実態に迫る。

### ATL細胞のDNAメチル化の異常

ATL研究におけるDNAメチル化についての最初の報告は、細胞周期調節遺伝子*CDKN2*ファミリーである。*CDKN2* locusにはp16, p14, p15という細胞周期の抑制にかかわる蛋白質がコードされており、他の腫瘍細胞においてもゲノム、エピゲノム異常の hotspotである。われわれが最近行ったATL患者のコピーナンバー解析でも168例中46例(27%)の症例でゲノムの欠失が蓄積していることがわかった<sup>4)</sup>。Nosakaらによるbisulfite sequencing解析では、急性型47%、リンパ腫型73%の症例でDNAのメチル化が検出され、慢性型17%、くすぶり型17%と比較して高いことが報告されている<sup>6)</sup>。また、このメチル化が*CDKN2A*遺伝子の転写に抑制的に働くことが示されている。また無症候性キャリアや非感染者ではメチル化は検出されていない。一方Hofmannらはmethylation-specific PCR(MSP)によって、*CDKN2A*よりむしろ*CDKN2B*遺伝子に高頻度のメチル化を検出している<sup>7)</sup>。また最近では、ATLの進展とメチル化の獲得について検討され、上記の遺伝子に加えて、*HCAD*, *SHP1*, *DAPK*などにお

けるDNAメチル化の獲得が報告されている<sup>8)</sup>。またこれらのメチル化の度合いと予後との相関も示唆されていることから、DNAメチル化と腫瘍細胞の悪性度にも関連がありそうである。しかし、われわれが行ったATL検体を用いた大規模な発現解析では、*CDKN2*ファミリーの発現減少は検出されおらず、実際のATL細胞における細胞周期調節遺伝子の機能と発現レベルについては今後詳細な検討が必要である。また最近になって*CDKN1A*遺伝子がATL細胞でDNAのメチル化によって抑制されていると報告された<sup>9)</sup>。*CDKN1A*(*p21<sup>waf1/Cip1</sup>*) mRNAはATL検体の発現解析でも減少を示しており<sup>4)</sup>、ATLにおけるDNAメチル化異常と細胞周期制御の破綻の関連が予想される。

細胞周期関連以外では、*BMP6*遺伝子のプロモーター領域のメチル化が報告されている。急性型96%、リンパ腫型94%、慢性型44%、くすぶり型20%と病型が進行に合わせて高頻度のメチル化が検出されている<sup>10)</sup>。また同一患者における慢性型から急性型への進展においても、*BMP6*のメチル化が誘導されており、ATLの予後や腫瘍細胞への機能的な影響が考えられる。また*APC*遺伝子についてもATL検体でDNAのメチル化が報告されている<sup>11)</sup>。固形がんや他の悪性リンパ腫において、これらの遺伝子のDNAのメチル化によるがん抑制機能の低下が報告されており、ATL細胞に

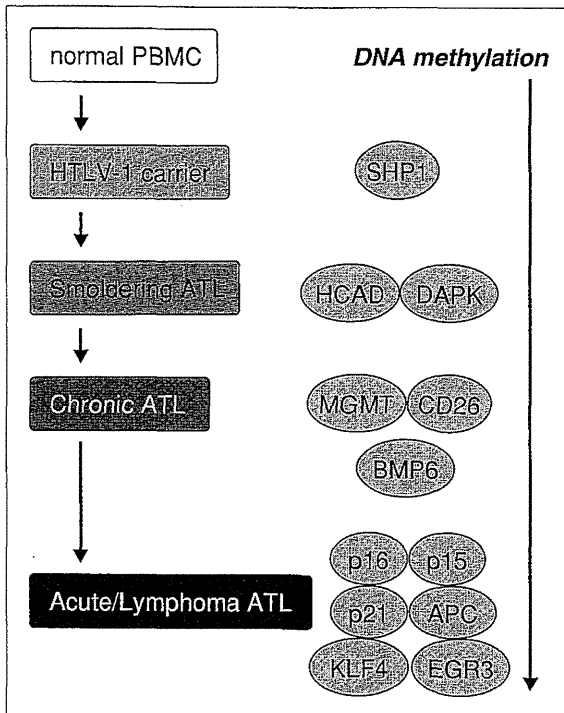


図2 ATLにおけるDNAメチル化の変遷  
個々の解析結果を図示した。感染細胞からATL細胞への過程でさまざまな遺伝子のメチル化が獲得される。メチル化された遺伝子は発現が抑制され、細胞周期制御の破綻やアポトーシス抵抗性に寄与する。

においても機能的な検討が必要であろう。

ATLの進行に伴う遺伝子発現の減少としてはCD26遺伝子が知られている。この表面マーカーはATL腫瘍細胞で発現が欠失しており、正常Tリンパ球との区別に有用であるが、このCD26遺伝子の発現減少にDNAメチル化がかかわっていることが報告されており<sup>12)</sup>、病気の進行に伴うDNAのメチル化の獲得が示唆されている。

Methylated CpG-island amplification/representational difference analysis (MCA/RDA) によるDNAのメチル化サイトと脱メチル化サイトのスクリーニングにより、Yasunagaらは53遺伝子の異常なDNAメチル化を明らかにしている<sup>13)</sup>。その中には、*KLF4*や*EGR3*といったアポトーシス抵抗性遺伝子が含まれている。また逆にDNAの脱メチル化についても、同研究グループは*MEL1*遺伝子のalternative splicing遺伝子である*MEL1S*が異常な脱メチル化によってATL細胞で発現していることを明らかにしている<sup>14)</sup>。また*MEL1S*の発現はT細胞株のTGF- $\beta$ による増殖抑制を阻害することを示している。

以上より、DNAメチル化のパターンの変化はATL細胞の分子レベルの特徴の一つであり、そのことが細胞レベルの特性に関与していることも明らかである(図2)。しかし前述のとおりDNAメチル化の全体的な解析は行われておらず、またDNAメチル化の制御にかかわる遺伝子異常も報告されていない。近年の網羅的解析技術を駆使して、腫瘍細胞の特徴にかかわるDNAのメチル化パターンを明らかにすることが今後の重要なポイントである。

### ATLにおけるヒストン修飾の異常

ヒストンの化学修飾は非常に多くのバリエーションがあり、ATLにおいても複雑な制御機構の逸脱が予想されているが、メチル化DNA解析に比べて臨床検体の調製の難易度が高く、したがって全体的な回答は得られていない。しかし、研究が先行しているヒストン脱アセチル化酵素(HDAC)については、その異常と細胞特性への関与が報告されている。

エピジェネティックな解析で強力なツールとなるのが阻害剤による検討である。Nishiokaらは複数のHDAC阻害剤を用いてHTLV-1感染細胞株を評価し、アポトーシスが誘導されることを明らかにしている<sup>15)</sup>。興味深いことにHTLV-1感染細胞で恒常的に活性化しているNF- $\kappa$ B経路がHDAC阻害剤の処理によって抑制されると報告している。しかしHDAC阻害剤は、NF- $\kappa$ B経路のRelAのアセチル化を誘導することによって逆に活性化させるという報告もあり<sup>16)</sup>、詳しい分子メカニズムの解析が必要である。

CpGアイランドを持つ遺伝子の多くは、実際にはヒストンのアセチル化とDNAのメチル化が協調して遺伝子発現を抑制することが多い。たとえばTBP-2遺伝子はHTLV-1感染細胞のtransformationの過程で、DNAのメチル化とヒストンの脱アセチル化によって発現が抑制される遺伝子である<sup>17)</sup>。TBP-2はHTLV-1感染細胞の増殖を抑制することから<sup>18)</sup>、ATL細胞の増殖能に対してエピジェネティックな脱制御が直接的にかかわっていると考えられる。最近新しいHDAC阻害剤であるAR42がATLのマウスモデルに対して有効であることが報告された<sup>19)</sup>。毒性の試験や標的遺伝

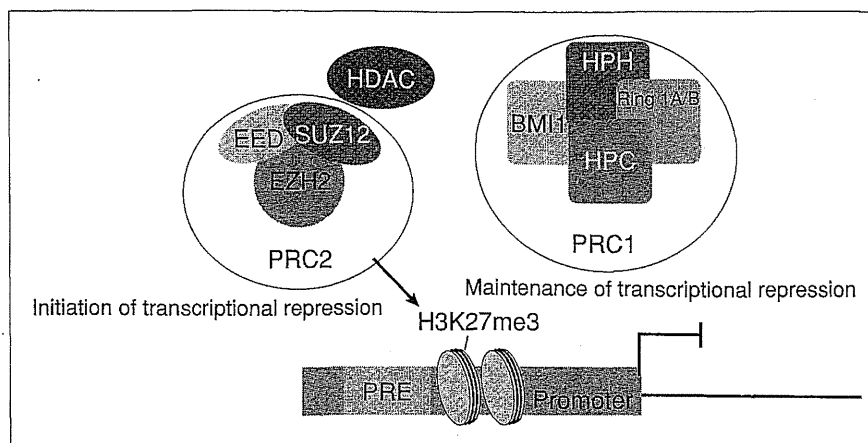


図3 Polycombファミリーによる遺伝子発現制御機構  
PRC1とPRC2によりプロモーター上のヒストンH3K27のメチル化が制御され、クロマチンの凝集が起こり、遺伝子発現が抑制される。

子の同定を含む詳細な分子メカニズムの解明が待たれる。

アセチル化に加えて、最近のがん研究において特に研究が進められているのが、ヒストンH3K27のメチル化である。これは、制御する因子群の発現異常や遺伝子変異が多くのがんで同定されていることに起因する。乳がんや前立腺がんなどの固形腫瘍に加え、多くのB細胞リンパ腫において、腫瘍細胞の生存、増殖、脱分化、転移浸潤能と相関することが知られている<sup>20)</sup>。H3K27のトリメチル化は主にユークロマチン領域において遺伝子発現の抑制マーカーとして機能する。PolycombファミリーはH3K27のメチル化を制御する因子群であり、これまで長年の研究から、Polycomb repressive complex 1 (PRC1) と PRC2 という別の複合体がそれぞれ、抑制クロマチン構造の維持と、メチル化導入の役割を担っている(図3)<sup>21)</sup>。また、細胞の分化に深くかかわっている分子群として同定されており、造血幹細胞の制御にも重要である。

ATLにおけるPolycombファミリーの異常は、網羅的遺伝子発現解析によって明らかにされた<sup>4)22)</sup>。なかでもH3K27のメチル化酵素であるEZH2の過剰発現が顕著であり、細胞全体のメチル化H3K27me3レベルの亢進も検出されている。EZH2の阻害剤であるDZNep処理によりATL細胞株のアポトーシスが誘導されることから、Polycombの発現異常がATL細胞の生存にかかわることが示されている<sup>22)</sup>。またHDAC阻害剤との併

用がより効果的であったことは、複雑なエピゲノムの脱制御がATL細胞の背景にあることを示唆している。

### ATL細胞のエピゲノム異常と細胞生存シグナルへの関与

われわれはATL細胞の分子病態の全体像をつかむために、HTLV-1感染者コホート共同研究班(JSPFAD)の全面的協力を得て、ATL 52例と健常人CD4陽性T細胞21例の網羅的遺伝子発現解析を行った。加えて、miRNA発現およびゲノムDNAコピー数の大規模な統合解析を行うことによって、ATL細胞の分子レベルの全体像をデータとして取得することに成功した<sup>4)</sup>。

ATLにおいて、Polycombファミリーに属する遺伝子群で顕著に異常を示したのが、EZH2およびSUZ12であった(表1)。いずれもPRC2の構成因子であり、その過剰発現はPRC2の酵素活性を上昇させ、異常なメチル化パターンが誘導されることが他の腫瘍で報告されている。われわれはさらに、これらの生物学的意義を明らかにするために多角的に検証した結果、ATL細胞におけるPolycombファミリーの発現異常ががん抑制性miRNAのサイレンシングにかかわっていることを明らかにした。

miRNAは遺伝子発現全体に対して“Fine tuner”として機能する分子群であり、がんやウイルス感染症を考える上でも欠かすことのできない因子として位置づけられている。miRNAによる遺

表 1 ATL細胞におけるPolycombファミリーの発現変化

Gene (PcG subunits)	PcG subunits in <i>Drosophila melanogaster</i>	PcG complex in humans	Fold change (ATL/Normal)	P value	
CBX2	Polycomb	PRC1	—	—	
CBX4			1.648	$1.09 \times 10^{-6}$	
CBX6			0.828	0.00258	
CBX7			—	—	
CBX8			2.363	$4.80 \times 10^{-9}$	
PHC1	Polyhomeotic		2.031	$1.19 \times 10^{-5}$	
PHC2			1.389	$9.45 \times 10^{-5}$	
BMI1	Posterior Sex combs		1.584	$5.01 \times 10^{-6}$	
MEL18			—	—	
NSPC1			—	—	
RING1	Sex combs extra		—	—	
RING1B			0.646	$1.36 \times 10^{-6}$	
EZH1	Enhancer of Zeste		PRC2	—	—
EZH2				2.827	$1.90 \times 10^{-15}$
SUZ12	Suppressor of Zeste 12			2.049	$4.94 \times 10^{-16}$
EED	Extra Sex combs	1.465 (EED2)		$3.29 \times 10^{-7}$	
RbAp48	Nucleosome remodeling factor 55	1.605		$1.25 \times 10^{-9}$	
RbAp46		1.245		0.00248	
PHF1	Polycomb-like	—		—	
MTF2		—		—	
PHF19		—		—	
YY1	Pleiohomeotic	PHORC		—	—
RYBP				1.681	$2.70 \times 10^{-6}$

ATL検体を用いた網羅的遺伝子発現解析の結果、正常CD4陽性T細胞と比較した発現量の変化を示した。(文献<sup>4)</sup>から引用、一部改変)

伝子発現制御機構の詳細は他の文献を参考されたい<sup>23)</sup>。特筆すべきは、miRNAの存在が示されて以降、遺伝子発現制御研究は飛躍的に進展したことである。

ATL, HTLV-1関連分野においてもmiRNAの異常が示唆されていたが、その実態は不明であった。われわれはATL細胞の分子病態の全体像をつかむために、ATL 40例、健常人CD4陽性T細胞 22例についてmiRNAの網羅的解析を行った結果、ATLでは61種のmiRNAが異常発現を示し、そのうち59種のmiRNAが正常T細胞に比べて低値を示すことがわかった。これは、腫瘍細胞はmiRNAの発現が全体的に低下傾向にあるという他のがん研究の結果と一致している。これらのmiRNAはATL細胞の新たな分子マーカーであり、またひとつひとつが腫瘍細胞の特徴に寄与していると考えられる。

61種の発現異常miRNAのうち、miR-31が例外なくすべてのATL患者で著しく減少していた(図4)。miR-31の発現減少は、乳がんにおける転移、

浸潤過程において重要であることが報告されている<sup>24)</sup>。われわれは、miR-31の著しい減少がATL細胞の特徴を反映していると考え、ATL細胞のmRNA発現プロファイルの結果と統合し、さらに*in vitro*の複数の実験を経て、ATL細胞におけるNF- $\kappa$ B活性化の原因遺伝子であるNIKがmiR-31の新規標的遺伝子であることを見出した。実験の結果、正常T細胞ではmiR-31の発現が比較的高くNIKの発現を抑制しているが、miR-31の異常な発現低下がNIKの発現誘導とそれに伴うNF- $\kappa$ B経路の恒常的活性化を誘発することがわかった。さらにATL細胞株および新鮮ATL細胞に対してmiR-31を再導入すると細胞死が誘導された。このことは、miR-31の細胞内レベルが腫瘍細胞の表現型に直接影響していることを意味し、新しい分子標的としての有用性が示された。

ATL臨床検体を詳細に解析した結果、ゲノムの欠損と上述したPolycombファミリー依存的なエピジェネティックな異常によって、miR-31の発現欠失がすべてのATL患者で起こっていることが

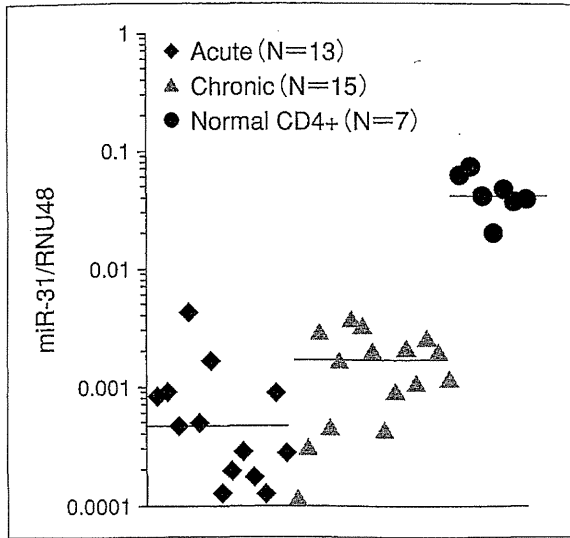


図4 ATLにおけるmiR-31の発現低下  
Real-time PCRによるmiR-31の定量結果. miR-31の発現は例外なくATLで発現が低下している.

わかった. さらに, PolycombファミリーがmiR-31を抑制することによってNIK-NF-κB経路を活性化する分子機構は, ATLだけでなく乳がん細胞やB細胞における免疫応答反応においても保存されていた. Polycombファミリー, NF-κB経路, miR-31はそれぞれが単独で, おおの多彩な機能によって細胞の恒常性や分化などのさまざまなプロセスにかかわると同時に, さらにクロストークを形成することによって, より複雑な遺伝子発現制御ネットワークを形成していると考えられる(図5)<sup>4)</sup>. われわれの実験結果は, 長らく不明であったATL細胞におけるNF-κB経路の恒常的活性化の詳細な分子機構を明らかにした<sup>3)</sup>. ATL細胞はこの分子ネットワークの異常に依存しており, Polycombの制御, もしくはmiR-31の補充による新たな治療法の開発につながると期待される.

Polycombファミリーについては, 造血器腫瘍において非常に盛んに研究が進められている分子群である. ほとんどすべてのB細胞リンパ腫において過剰に発現しており<sup>25)</sup>, またさらに一部の腫瘍においてはgain-of-function mutationも報告されていることもあり, 治療標的としても注目を浴びている<sup>26)</sup>. しかし一方で未分化な白血病細胞では逆にがん抑制性遺伝子として機能していることも明らかとなり<sup>27)</sup>, 分化段階とPolycombによるエピジェネティック制御は今後さらに研

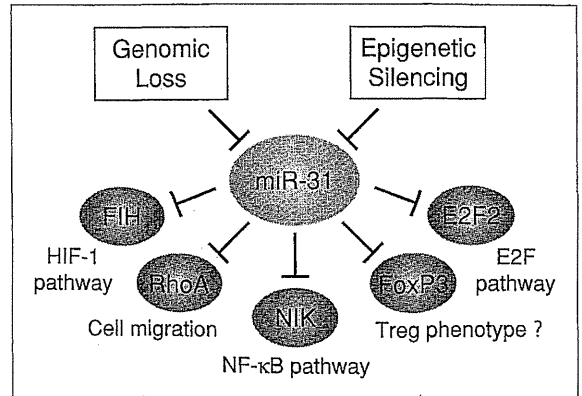


図5 ATL細胞における新たな分子メカニズム  
遺伝子の欠損とPolycomb依存的なエピジェネティックな異常によってmiR-31の発現が低下すると, NIKなどの標的遺伝子の発現抑制が解除され, 細胞内のシグナル伝達経路が攪乱される. この分子メカニズムは他のがん細胞でも保存されている.

究が加速すると考えられる.

### HTLV-1感染による 宿主エピゲノムへの影響

ATL細胞のエピゲノムの異常の実態が少しずつ明らかになっている一方で, どのような過程を経て異常パターンを獲得するのかについてはほとんど明らかではない. しかし実験的証拠として, ウイルス遺伝子産物であるTaxが宿主T細胞のエピジェネティック調節因子に結合し, 影響を与えることが複数示されている.

TaxはHDAC1と相互作用し, プロウイルスの制御を担うと同時に, 宿主に対しても影響を与えることが示唆されている<sup>28)</sup>. またわれわれはTaxとヒストンメチル化酵素であるSUV39H1やSMYD3との物理的な相互作用を発見した<sup>29)30)</sup>. 終末像であるATL細胞のエピゲノムの異常の維持と特性を明らかにするとともに, HTLV-1感染細胞からATL細胞への進展を考える上で, 包括的なエピゲノム解析と詳細な分子機構の解明が急務であろう.

### 今後の展望

ゲノム, エピゲノムの異常を背景として, 細胞周期の脱制御, miRNAの発現低下, シグナル伝達経路の恒常的活性化がこれまでに明らかになっているATL細胞の分子レベルの特徴である(図6). miRNAの全体的な発現低下に対して, エピゲノ



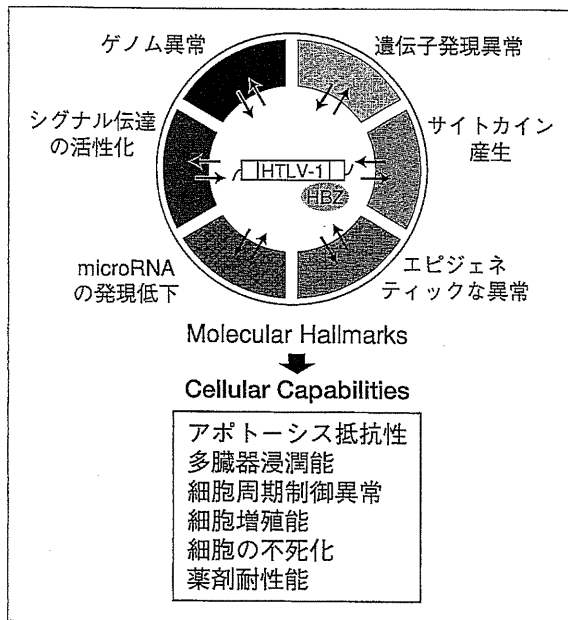


図6 ATL細胞における分子レベルの特徴  
大規模解析結果からみるATLの分子レベルの特徴を概略図として示した。HTLV-1感染細胞がさまざまな分子異常を獲得し、悪性度の高い腫瘍細胞の特徴に寄与する。(文献<sup>3)</sup>より引用、一部改変)

ムの脱制御がどのようにかかわっているのかは、非常に興味深い課題である。今後は、これまでの感染細胞株や終末像である新鮮ATL細胞の詳細なデータをまとめ、感染細胞の恒常性の破綻、感染クローンの変遷、発症や薬剤耐性の分子メカニズム、などに対するエピゲノムの異常のかかわりについて取り組む必要があるであろう。

## 文 献

- 1) Yamaguchi K, Watanabe T. Human T lymphotropic virus type-I and adult T-cell leukemia in Japan. *Int J Hematol* 2002 ; 76 Suppl 2 : 240.
- 2) Matsuoka M, Jeang KT. Human T-cell leukaemia virus type 1 (HTLV-1) infectivity and cellular transformation. *Nat Rev Cancer* 2007 ; 7 : 270.
- 3) Yamagishi M, Watanabe T. Molecular hallmarks of adult T cell leukemia. *Front Microbiol* 2012 ; 3 : 334.
- 4) Yamagishi M, Nakano K, Miyake A, et al. Polycomb-mediated loss of miR-31 activates NIK-dependent NF- $\kappa$ B pathway in adult T cell leukemia and other cancers. *Cancer Cell* 2012 ; 21 : 121.
- 5) Yamagishi M, Watanabe T. New paradigm of T cell signaling : learning from malignancies. *J Clin Cell Immunol* 2012 ; S12 : 007.
- 6) Nosaka K, Maeda M, Tamiya S, et al. Increasing methylation of the CDKN2A gene is associated with the progression of adult T-cell leukemia. *Cancer Res* 2000 ; 60 : 1043.
- 7) Hofmann WK, Tsukasaki K, Takeuchi N, et al. Methylation analysis of cell cycle control genes in adult T-cell leukemia/lymphoma. *Leuk Lymphoma* 2001 ; 42 : 1107.
- 8) Sato H, Oka T, Shinnou Y, et al. Multi-step aberrant CpG island hyper-methylation is associated with the progression of adult T-cell leukemia/lymphoma. *Am J Pathol* 2010 ; 176 : 402.
- 9) Watanabe M, Nakahata S, Hamasaki M, et al. Downregulation of CDKN1A in adult T-cell leukemia/lymphoma despite overexpression of CDKN1A in human T-lymphotropic virus 1-infected cell lines. *J Virol* 2010 ; 84 : 6966.
- 10) Taniguchi A, Nemoto Y, Yokoyama A, et al. Promoter methylation of the bone morphogenetic protein-6 gene in association with adult T-cell leukemia. *Int J Cancer* 2008 ; 123 : 1824.
- 11) Yang Y, Takeuchi S, Tsukasaki K, et al. Methylation analysis of the adenomatous polyposis coli (APC) gene in adult T-cell leukemia/lymphoma. *Leuk Res* 2005 ; 29 : 47.
- 12) Tsuji T, Sugahara K, Tsuruda K, et al. Clinical and oncologic implications in epigenetic down-regulation of CD26/dipeptidyl peptidase IV in adult T-cell leukemia cells. *Int J Hematol* 2004 ; 80 : 254.
- 13) Yasunaga J, Taniguchi Y, Nosaka K, et al. Identification of aberrantly methylated genes in association with adult T-cell leukemia. *Cancer Res* 2004 ; 64 : 6002.
- 14) Yoshida M, Nosaka K, Yasunaga J, et al. Aberrant expression of the MEL1S gene identified in association with hypomethylation in adult T-cell leukemia cells. *Blood* 2004 ; 103 : 2753.
- 15) Nishioka C, Ikezoe T, Yang J, et al. Histone deacetylase inhibitors induce growth arrest and apoptosis of HTLV-1-infected T-cells via blockade of signaling by nuclear factor kappaB. *Leuk Res* 2008 ; 32 : 287.

- 16) Chiechio S, Zammataro M, Morales ME, et al. Epigenetic modulation of mGlu2 receptors by histone deacetylase inhibitors in the treatment of inflammatory pain. *Mol Pharmacol* 2009 ; 75 : 1014.
- 17) Ahsan MK, Masutani H, Yamaguchi Y, et al. Loss of interleukin-2-dependency in HTLV-I-infected T cells on gene silencing of thioredoxin-binding protein-2. *Oncogene* 2006 ; 25 : 2181.
- 18) Nishinaka Y, Nishiyama A, Masutani H, et al. Loss of thioredoxin-binding protein-2/vitamin D3 up-regulated protein 1 in human T-cell leukemia virus type I-dependent T-cell transformation : implications for adult T-cell leukemia leukemogenesis. *Cancer Res* 2004 ; 64 : 1287.
- 19) Zimmerman B, Sargeant A, Landes K, et al. Efficacy of novel histone deacetylase inhibitor, AR42, in a mouse model of, human T-lymphotropic virus type 1 adult T cell lymphoma. *Leuk Res* 2011 ; 35 : 1491.
- 20) Sparmann A, van Lohuizen M. Polycomb silencers control cell fate, development and cancer. *Nat Rev Cancer* 2006 ; 6 : 846.
- 21) Schuettengruber B, Chourrout D, Vervoort M, et al. Genome regulation by polycomb and trithorax proteins. *Cell* 2007 ; 128 : 735.
- 22) Sasaki D, Imaizumi Y, Hasegawa H, et al. Overexpression of Enhancer of zeste homolog 2 with trimethylation of lysine 27 on histone H3 in adult T-cell leukemia/lymphoma as a target for epigenetic therapy. *Haematologica* 2011 ; 96 : 712.
- 23) He L, Hannon GJ. MicroRNAs : small RNAs with a big role in gene regulation. *Nat Rev Genet* 2004 ; 5 : 522.
- 24) Valastyan S, Reinhardt F, Benaich N, et al. A pleiotropically acting microRNA, miR-31, inhibits breast cancer metastasis. *Cell* 2009 ; 137 : 1032.
- 25) Martin-Perez D, Piris MA, Sanchez-Beato M. Polycomb proteins in hematologic malignancies. *Blood* 2010 ; 116 : 5465.
- 26) McCabe MT, Ott HM, Ganji G, et al. EZH2 inhibition as a therapeutic strategy for lymphoma with EZH2-activating mutations. *Nature* 2012 ; 492 : 108.
- 27) Hock H. A complex Polycomb issue : the two faces of EZH2 in cancer. *Genes Dev* 2012 ; 26 : 751.
- 28) Ego T, Ariumi Y, Shimotohno K. The interaction of HTLV-1 Tax with HDAC1 negatively regulates the viral gene expression. *Oncogene* 2002 ; 21 : 7241.
- 29) Kamoi K, Yamamoto K, Misawa A, et al. SUV39H1 interacts with HTLV-1 Tax and abrogates Tax transactivation of HTLV-1 LTR. *Retrovirology* 2006 ; 3 : 5.
- 30) Yamamoto K, Ishida T, Nakano K, et al. SMYD3 interacts with HTLV-1 Tax and regulates subcellular localization of Tax. *Cancer Sci* 2011 ; 102 : 260.

\* \* \*

for patients who fail high dose chemoradiotherapy and autologous stem cell rescue for relapsed and primary refractory Hodgkin lymphoma. *British Journal of Haematology*, **146**, 158–163.

Moskowitz, A.J., Hamlin, P.A., Perales, M.A., Gerecitano, J., Horwitz, S.M., Matasar, M.J., Noy, A., Palomba, M.L., Portlock, C.S., Straus, D.J., Graustein, T., Zelenetz, A.D. & Moskowitz, C.H. (2013) Phase II study of bendamustine in

relapsed and refractory Hodgkin lymphoma. *Journal of Clinical Oncology*, **31**, 456–460.

Younes, A., Oki, Y., Bociek, R.G., Kuruvilla, J., Fanale, M., Neelapu, S., Copeland, A., Buglio, D., Galal, A., Besterman, J., Li, Z., Drouin, M., Patterson, T., Ward, M.R., Paulus, J.K., Ji, Y., Medeiros, L.J. & Martell, R.E. (2011) Mocetinostat for relapsed classical Hodgkin's lymphoma: an open-label, single-arm, phase 2 trial. *The Lancet Oncology*, **12**, 1222–1228.

Zinzani, P.L., Viviani, S., Anastasia, A., Vitolo, U., Luminari, S., Zaja, F., Corradini, P., Spina, M., Brusamolino, E., Gianni, A.M., Santoro, A., Botto, B., Derenzini, E., Pellegrini, C. & Argnani, L. (2013) Brentuximab vedotin in relapsed/refractory Hodgkin's lymphoma: Italian experience and results of the use in the daily clinic outside clinical trials. *Haematologica*, **98**, 1232–1236.

## Loss of CCR4 antigen expression after mogamulizumab therapy in a case of adult T-cell leukaemia-lymphoma

Adult T-cell leukaemia-lymphoma (ATL) is an aggressive peripheral T-cell neoplasm caused by human T-cell leukaemia virus type I infection. Most cases of aggressive ATL (acute, lymphoma, or unfavourable chronic type) are resistant to conventional chemotherapeutic agents, and, thus, it has a poor prognosis (Shimoyama, 1991; Tsukasaki *et al*, 2007). Therefore, development of alternative treatment strategies is an urgent issue. CC chemokine receptor 4 (CCR4) is expressed on most ATL cells and has been shown to be a new molecular target of immunotherapy *in vivo* (Ito *et al*, 2009). Mogamulizumab, a novel molecular targeting agent, is a humanized anti-CCR4 immunoglobulin G1 monoclonal antibody with a defucosylated Fc region, and 50% efficacy has been shown as a single agent in a phase II study for relapsed and refractory ATL (Ishida *et al*, 2012). We have little experience with this agent, as large-scale clinical studies have not been conducted. Here, we report an acute ATL case whose tumour cells lost CCR4 expression after administration of mogamulizumab.

A 63-year-old female was admitted to our hospital for fatigue, fever, skin eruption and hypercalcaemia, and was diagnosed with acute-type ATL. We started a dose-intensified chemotherapy of VCAP-AMP-VECP (vincristine, cyclophosphamide, doxorubicin, and prednisone; doxorubicin, ranimustine, and prednisone; and vindesine, etoposide, carboplatin, and prednisone) immediately. Six cycles were carried out, and partial remission was obtained, but the ATL cells remained in peripheral blood and skin lesions. ATL recurred with skin lesions immediately while myelosuppression was prolonged. Therefore, we started administration of mogamulizumab as a single agent, once per week for 8 weeks at a dose of 1.0 mg/kg. By the end of the treatment, complete remission was obtained with disappearance of ATL cells in peripheral blood, skin lesions, and normalization of lactate dehydrogenase levels. Unfortunately, a similar eruption developed approximately 3 months later, and the ATL relapsed. The patient again underwent mogamulizumab therapy, as she did not want further chemotherapy. However, the

second administration had no effect, and the patient died due to disease progression.

We analysed CCR4 expression on patient ATL cells using multi-colour flow cytometry analysis, as described previously (Tian *et al*, 2011) to reveal the resistance mechanism. After dead cells (propidium iodide positive) and monocytes (CD4<sup>dim</sup> CD14<sup>+</sup>) were gated out, a CD3 vs. CD7 plot of CD4<sup>+</sup> T cells was constructed, and CCR4 expression on the CD3<sup>dim</sup>/CD7<sup>low</sup> subpopulation, in which ATL cells were highly enriched, was analysed. This analysis clearly revealed loss of CCR4 expression on ATL tumour cells after mogamulizumab therapy (Fig 1). Furthermore, we conducted clonal analysis by

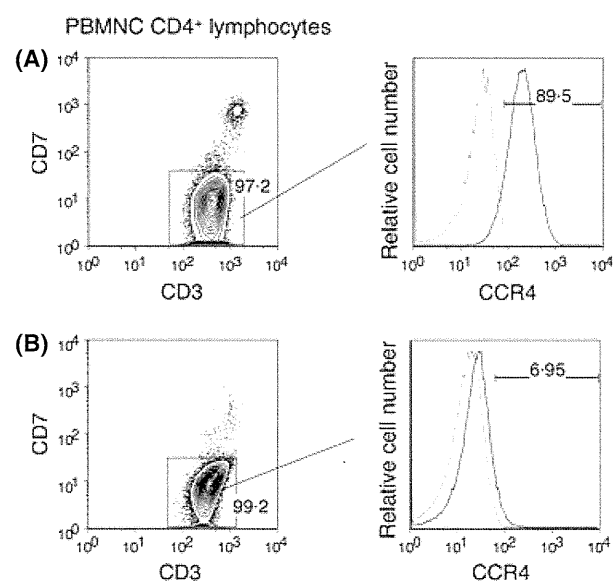


Fig 1. Multicolour flow cytometric analysis of CCR4 expression on adult T-cell leukaemia-lymphoma (ATL) cells. (A) Before mogamulizumab therapy. (B) After second mogamulizumab therapy. The ATL cells accumulated a CD7<sup>low</sup> subpopulation before and after treatment, without any change. Loss of the CC chemokine receptor 4 (CCR4) antigen was clearly observed after treatment. PBMNC, peripheral blood mononuclear cells.

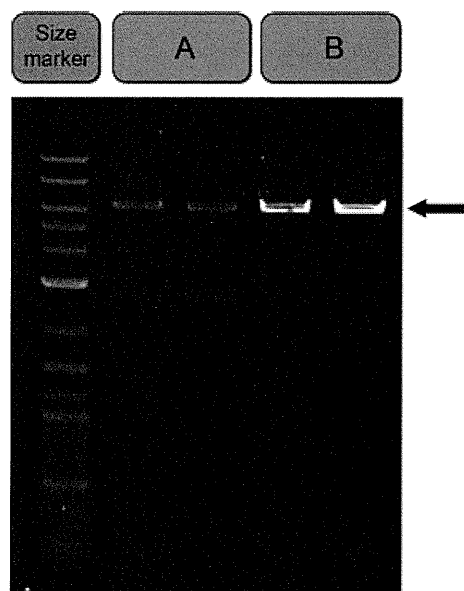


Fig 2. Clonal analysis by inverse long polymerase chain reaction (duplicated). (A) Before mogamulizumab therapy. (B) After second mogamulizumab therapy. The same monoclonal bands were observed before and after mogamulizumab therapy (arrow).

inverse long polymerase chain reaction (PCR) using the same sample. Genomic DNA extracted from peripheral blood mononuclear cells was digested with PstI. The purified DNA was self-ligated with T4 DNA ligase (Takara Bio, Otsu, Japan) and inverse long PCR was performed using Tks Gflex DNA Polymerase (Takara Bio) (Kobayashi *et al*, 2013). The PCRs were performed in duplicate. The band of the major clone was of identical size before and after mogamulizumab therapy (Fig 2), suggesting that the relapsed CCR4<sup>-</sup> ATL cells belonged to the same clone as the original CCR4<sup>+</sup> ATL cells.

To the best of our knowledge, this is the first report of loss of the CCR4 antigen by clonal analysis after mogamulizumab therapy. The resistance mechanism to mogamulizumab has not been elucidated to date. Mogamulizumab exerts its activity on CCR4-expressing T cells through an indirect effector mechanism, antibody-dependent cell-mediated cytotoxicity (ADCC) (Ishii *et al*, 2010). Thus, the CCR4 molecule itself could be involved in the resistance to mogamulizumab by loss of expression. It is believed that target molecular loss is not a rare phenomenon during monoclonal antibody therapy. For example, several reports are available regarding the loss of CD20 expression after the administration of rituximab, which is an anti-CD20 monoclonal antibody (Duman *et al*, 2012). Several mechanisms ranging from the gene to the protein level have been proposed to explain loss of CD20; a similar mechanism might cause loss of CCR4 expression. We demonstrated loss of CCR4 expression on the same ATL clone, which excluded the possibility of a clonal change by CCR4<sup>-</sup> ATL cells after mogamulizumab treatment. We have experienced another

patient who became resistant to a second mogamulizumab administration but whose ATL cells maintained CCR4 expression. Loss of CCR4 expression is one of the resistance mechanisms to mogamulizumab; others include mutation or deletion within epitope-coding regions for mogamulizumab, increase in soluble CCR4, and reduced ADCC.

The anti-CCR4 antibody used in this study, clone 1G1, recognizes a distinct epitope from mogamulizumab (Ishii *et al*, 2010), which excluded the possibility of epitope masking by mogamulizumab. Our results indicate that CCR4 expression by ATL cells should be re-evaluated when relapsed patients with ATL are treated after mogamulizumab therapy even if their tumour cells express CCR4 at the initial evaluation.

### Acknowledgements

We thank Ms. Eri Watanabe (Institute of Medical Science, The University of Tokyo) for technical assistance with flow cytometry. We are grateful to the hospital staff who are committed to providing high-quality care for all of our patients.

### Author contributions

NO and KU wrote the manuscript. SK and TI performed the experiments using patient samples. KY, MK, and KS provided patient care and clinical information. NW supervised the flow cytometry. NO, AT, and KU supervised the research; and all authors approved the final manuscript.

### Conflict of interest

The authors declare no financial conflict of interest.

Nobuhiro Ohno<sup>1</sup>  
 Seiichiro Kobayashi<sup>2</sup>  
 Tomohiro Ishigaki<sup>2</sup>  
 Koichiro Yuji<sup>1</sup>  
 Masayuki Kobayashi<sup>2</sup>  
 Koota Sato<sup>2</sup>  
 Nobukazu Watanabe<sup>3</sup>  
 Arinobu Tojo<sup>1,2</sup>  
 Kaoru Uchamaru<sup>1</sup>

<sup>1</sup>Department of Haematology/Oncology, Research Hospital, The Institute of Medical Science, The University of Tokyo, <sup>2</sup>Division of Molecular Therapy, The Institute of Medical Science, The University of Tokyo, and <sup>3</sup>Laboratory of Diagnostic Medicine, Division of Stem Cell Therapy, The Institute of Medical Science, The University of Tokyo, Tokyo, Japan  
 E-mail: nobuohno@ims.u-tokyo.ac.jp

**Keywords:** adult T-cell leukaemia-lymphoma, mogamulizumab, CC chemokine receptor 4, monoclonal antibody, flow cytometry

First published online 3 September 2013

doi: 10.1111/bjh.12555

## References

- Duman, B.B., Sahin, B., Ergin, M. & Guvenc, B. (2012) Loss of CD20 antigen expression after rituximab therapy of CD20 positive B cell lymphoma (diffuse large B cell extranodal marginal zone lymphoma combination): a case report and review of the literature. *Medical Oncology*, **29**, 1223–1226.
- Ishida, T., Joh, T., Uike, N., Yamamoto, K., Utsunomiya, A., Yoshida, S., Saburi, Y., Miyamoto, T., Takemoto, S., Suzushima, H., Tsukasaki, K., Nosaka, K., Fujiwara, H., Ishitsuka, K., Inagaki, H., Ogura, M., Akinaga, S., Tomonaga, M., Tobinai, K. & Ueda, R. (2012) Defucosylated anti-CCR4 monoclonal antibody (KW-0761) for relapsed adult T-cell leukemia-lymphoma: a multicenter phase II study. *Journal of Clinical Oncology*, **30**, 837–842.
- Ishii, T., Ishida, T., Utsunomiya, A., Inagaki, A., Yano, H., Komatsu, H., Iida, S., Imada, K., Uchiyama, T., Akinaga, S., Shitara, K. & Ueda, R. (2010) Defucosylated humanized anti-CCR4 monoclonal antibody KW-0761 as a novel immunotherapeutic agent for adult T-cell leukemia/lymphoma. *Clinical Cancer Research*, **16**, 1520–1531.
- Ito, A., Ishida, T., Utsunomiya, A., Sato, F., Mori, F., Yano, H., Inagaki, A., Suzuki, S., Takino, H., Ri, M., Kusumoto, S., Komatsu, H., Iida, S., Inagaki, H. & Ueda, R. (2009) Defucosylated anti-CCR4 monoclonal antibody exerts potent ADCC against primary ATLL cells mediated by autologous human immune cells in NOD/Shi-scid, IL-2R gamma(null) mice in vivo. *Journal of Immunology*, **183**, 4782–4791.
- Kobayashi, S., Tian, Y., Ohno, N., Yuji, K., Ishigaki, T., Isobe, M., Tsuda, M., Oyaizu, N., Watanabe, E., Watanabe, N., Tani, K., Tojo, A. & Uchimaru, K. (2013) The CD3 versus CD7 plot in multicolor flow cytometry reflects progression of disease stage in patients infected with HTLV-I. *PLoS ONE*, **8**, 1–9.
- Shimoyama, M. (1991) Diagnostic criteria and classification of clinical subtypes of adult T-cell leukaemia lymphoma. A report from the Lymphoma Study Group (1984-87). *British Journal of Haematology*, **79**, 428–437.
- Tian, Y., Kobayashi, S., Ohno, N., Isobe, M., Tsuda, M., Zaïke, Y., Watanabe, N., Tani, K., Tojo, A. & Uchimaru, K. (2011) Leukemic T cells are specifically enriched in a unique CD3(dim) CD7 (low) subpopulation of CD4(+) T cells in acute-type adult T-cell leukemia. *Cancer science*, **102**, 569–577.
- Tsukasaki, K., Utsunomiya, A., Fukuda, H., Shibata, T., Fukushima, T., Takatsuka, Y., Ikeda, S., Masuda, M., Nagoshi, H., Ueda, R., Tamura, K., Sano, M., Momita, S., Yamaguchi, K., Kawano, F., Hanada, S., Tobinai, K., Shimoyama, M., Hotta, T., Tomonaga, M. & Japan Clinical Oncology Group Study JCOG9801. (2007) VCAP-AMP-VECP compared with biweekly CHOP for adult T-cell leukemia-lymphoma: Japan Clinical Oncology Group Study JCOG9801. *Journal of Clinical Oncology*, **25**, 5458–5464.

## Correlating prothrombin time with plasma rivaroxaban level

Recently published guidelines from the British Committee for Standards in Haematology suggest that the prothrombin time (PT) can be used for urgent determination of anticoagulation intensity with rivaroxaban if a reagent with a known sensitivity is used (Baglin *et al.*, 2012). However, it has been established in experiments using normal plasma spiked with varying concentrations of rivaroxaban that different PT reagents may have very different sensitivities to rivaroxaban (Samama *et al.*, 2010; Douxfils *et al.*, 2012). The clinical implications of this variation in PT sensitivity to rivaroxaban is evident from the recent report by Van Veen *et al.* (2013), who described normal PTs in the presence of therapeutic rivaroxaban levels in a patient with renal impairment. Comparing the PT using Innovin<sup>®</sup> (Siemens, Marburg, Germany) and Thromborel S<sup>®</sup> (Siemens) in a patient commenced on rivaroxaban 15 mg twice daily for deep vein thrombosis against the rivaroxaban plasma concentration measured by the Biophen DiXal anti-Xa assay, they demonstrated normal PT results despite therapeutic plasma rivaroxaban levels. They concluded that PT results should be interpreted with caution when assessing coagulation intensity for patients on rivaroxaban (Van Veen *et al.*, 2013). If available, a specific anti-Xa assay should be used for patients presenting with major bleeding or when requiring emergency surgery. Mueck *et al.* (2011) have also demonstrated variation using Neoplastine<sup>®</sup> (Diagnostica Stago, Asnieres-sur-Seine, France) to measure the PT against rivaroxaban concentration.

However, many coagulation laboratories will not have 24-h access to a rivaroxaban-calibrated anti-Xa assay and will

inevitably rely on their routine coagulation screen PT and activated partial thromboplastin time (APTT) results. Therefore it is essential that laboratories have knowledge of their reagents sensitivity to rivaroxaban. We studied the correlation between the rivaroxaban concentration (measured by Liquid Anti-Xa chromogenic assay, (Instrumentation Laboratory Company, Bedford, MA, USA) run on an IL TOP 700) and PT and APTT. The anti-Xa assay was calibrated using lyophilized standard rivaroxaban plasmas (Hyphen Biomed, Neuville-sur-Oise, France) to create a rivaroxaban assay linear between 0 and 400 ng/ml. Peak rivaroxaban plasma concentrations are considered to be in the range of 100–400 ng/ml, and trough concentrations in the range of 20–150 ng/ml (Baglin *et al.*, 2012). PT (Recombiplastin 2G<sup>®</sup>, Instrumentation Laboratory Company, laboratory reference range 9–13 s) and APTT (Synthasil<sup>®</sup>, Instrumentation Laboratory Company, laboratory reference range 27–38 s) were determined on the IL TOP 700.

Blood samples ( $n = 33$ ) were collected at random time points from 31 patients receiving rivaroxaban treatment for a minimum of 2 weeks. Fourteen results were obtained during 15 mg twice daily dosing and 19 during 20 mg once daily dosing. 19 blood samples were taken around the peak plasma concentration (1.0–5.5 h), 13 during trough periods (12–30 h) and for one patient, the sampling time was uncertain. The anti-Xa rivaroxaban concentrations during peak hours were marginally higher than was expected, with a median of 280 ng/ml (range 168–458). The trough levels were as expected, with a median of 57 ng/ml (range 11–215). There

# Adult T-cell leukemia cells are characterized by abnormalities of *Helios* expression that promote T cell growth

Satomi Asanuma,<sup>1</sup> Makoto Yamagishi,<sup>1</sup> Katsuaki Kawanami,<sup>1</sup> Kazumi Nakano,<sup>1</sup> Aiko Sato-Otsubo,<sup>2</sup> Satsuki Muto,<sup>2</sup> Masashi Sanada,<sup>2</sup> Tadanori Yamochi,<sup>1</sup> Seiichiro Kobayashi,<sup>3</sup> Atae Utsunomiya,<sup>4</sup> Masako Iwanaga,<sup>5</sup> Kazunari Yamaguchi,<sup>6</sup> Kaoru Uchimarui,<sup>3</sup> Seishi Ogawa<sup>2</sup> and Toshiki Watanabe<sup>1,7</sup>

<sup>1</sup>Graduate School of Frontier Sciences, The University of Tokyo; <sup>2</sup>Cancer Genomics Project, Graduate School of Medicine, The University of Tokyo; <sup>3</sup>Institute of Medical Science, The University of Tokyo, Tokyo; <sup>4</sup>Department of Hematology, Imamura Bun-in Hospital, Kagoshima; <sup>5</sup>Graduate School of Public Health, Teikyo University; <sup>6</sup>Department of Safety Research on Blood and Biological Products, National Institute of Infectious Diseases, Tokyo, Japan

(Received December 27, 2012/Revised April 11, 2013/Accepted April 15, 2013/Accepted manuscript online April 18, 2013/Article first published online May 19, 2013)

Molecular abnormalities involved in the multistep leukemogenesis of adult T-cell leukemia (ATL) remain to be clarified. Based on our integrated database, we focused on the expression patterns and levels of Ikaros family genes, *Ikaros*, *Helios*, and *Aiolos*, in ATL patients and HTLV-1 carriers. The results revealed profound deregulation of *Helios* expression, a pivotal regulator in the control of T-cell differentiation and activation. The majority of ATL samples (32/37 cases) showed abnormal splicing of *Helios* expression, and four cases did not express *Helios*. In addition, novel genomic loss in *Helios* locus was observed in 17/168 cases. We identified four ATL-specific short *Helios* isoforms and revealed their dominant-negative function. Ectopic expression of ATL-type *Helios* isoform as well as knockdown of normal *Helios* or *Ikaros* promoted T-cell growth. Global mRNA profiling and pathway analysis showed activation of several signaling pathways important for lymphocyte proliferation and survival. These data provide new insights into the molecular involvement of *Helios* function in the leukemogenesis and phenotype of ATL cells, indicating that *Helios* deregulation is one of the novel molecular hallmarks of ATL. (*Cancer Sci* 2013; 104: 1097–1106)

Adult T-cell leukemia (ATL) is a highly aggressive malignancy of mature CD4<sup>+</sup> T cells and is caused by HTLV-1. After HTLV-1 infection, ATL is thought to develop following a multitude of events, including both genetic and epigenetic changes in the cells. Although many aspects of HTLV-1 biology have been elucidated, the detailed molecular mechanism of ATL leukemogenesis remains largely unknown.<sup>(1,2)</sup> Therefore, to precisely define the comprehensive abnormalities associated with ATL leukemogenesis, we previously carried out global mRNA and miRNA profiling of ATL cells derived from a large number of patients.<sup>(3,4)</sup> In this study, we focused on Ikaros family genes, especially *Helios*, on the basis of our integrated profiling of expression and gene copy number in ATL cells, which revealed the deregulated expression of this family of genes and genomic loss of *Helios* locus.

Ikaros family genes are specifically expressed in the hematopoietic system and play a vital role in regulation of lymphoid development and differentiation.<sup>(5–11)</sup> In addition, they are known to function as tumor suppressors during leukemogenesis according to several genetic studies carried out in mouse models.<sup>(12–15)</sup> Recently, many studies reported the deregulated splicing of Ikaros and the deletion of *Ikaros* locus in several human leukemias.<sup>(16–23)</sup> These abnormalities are associated with poor prognoses.<sup>(24–27)</sup> *Helios* is mainly expressed in the T-cell lineage.<sup>(10,11)</sup> Genomic changes and abnormal expression of *Helios* are also observed in some

patients with T-cell malignancies.<sup>(18,28–31)</sup> However, in contrast to Ikaros, the substantial impact of aberrant *Helios* expression remains to be elucidated because of the absence of functional information, including the target genes of *Helios*.

In this study, we carried out a detailed expression analysis of Ikaros family genes in a large panel of clinical samples from ATL patients and HTLV-1 carriers and consequently identified a novel molecular characteristic, that is, abnormal splicing of *Helios* and loss of expression, which seems to be a significant key factor in leukemogenesis affecting the regulation of T-cell proliferation.

## Materials and Methods

**Cell lines and clinical samples.** HeLa and 293T cells were cultivated in DMEM supplemented with 10% FCS. Human leukemic T cells, Jurkat, Molt-4, and CEM, ATL-derived, MT-1 and TL-Om1, and HTLV-1-infected MT-2 and Hut-102 cell lines were all maintained in RPMI-1640 with 10% FCS. The PBMCs from ATL patients of four clinical subtypes<sup>(32)</sup> and healthy volunteers were a part of those collected with informed consent as a collaborative project of the Joint Study on Prognostic Factors of ATL Development. The project was approved by the Institute of Medical Sciences, University of Tokyo Human Genome Research Ethics Committee (Tokyo, Japan). Clinical information of ATL individuals is provided in Table S1.

**RNA isolation and RT-PCR analysis.** The preparation of total RNA and synthesis of the first strand of cDNA were described previously.<sup>(3)</sup> The mRNAs of Ikaros family genes were examined by PCR with Platinum Taq DNA Polymerase High Fidelity (Invitrogen, Carlsbad, CA, USA). The PCR products were sequenced by automated DNA sequencer. Nested PCR amplification was carried out with diluted full-length PCR products by Accuprime Taq DNA polymerase High Fidelity (Invitrogen). Quantitative PCR was carried out as previously described.<sup>(3)</sup> The specific primer sets for each PCR are described in Table S2.

**Immunoblot analysis.** Cells were collected, washed with PBS, and lysed with RIPA buffer. For immunoprecipitation, cells were lysed with TNE buffer and incubated with specific antibody. Proteins samples were then analyzed by immunoblots with specific antibodies: anti-tubulin, anti-Ikaros, and anti-*Helios* antibodies were from Santa Cruz Biotechnology (Santa Cruz, CA, USA). Mouse anti-FLAG antibody (M2) was from Sigma-Aldrich (St. Louis, MO, USA). Rabbit polyclonal anti-HA

<sup>7</sup>To whom correspondence should be addressed.  
E-mail: tnabe@ims.u-tokyo.ac.jp

antibody was from MBL (Nagoya, Japan). Anti-mouse, rabbit, and goat secondary antibodies were from Promega (Fitchburg, WI, USA).

**Immunostaining.** HeLa cells were cultured on coverslip slides and transfected with the indicated expression vectors by Lipofectamine LTX (Invitrogen). At 24 h post transfection, cells were washed three times with PBS, fixed in 4% paraformaldehyde, and permeabilized with 0.1% Triton X-100. Then, cells were stained with primary antibodies (diluted 1:500 to 1:2000). Alexa-488 or 546-conjugated secondary antibodies (Molecular Probes, Life Technologies, Carlsbad, CA, USA) were used for detection of specific targets, and DAPI was used for nuclear staining. Images were acquired by using a Nikon A1 confocal microscope (Nikon, Tokyo, Japan).

**Electrophoretic mobility-shift assay.** Experimental conditions and detail methods were previously reported.<sup>(3)</sup> For evaluation of DNA binding activity, 3–5  $\mu$ g nuclear extracts from each transfectant were used per each lane of electrophoresis. The oligonucleotide sequences used as a probe are provided in Table S2.

**Luciferase assay.** The pGL4.10-firefly vector (Promega) containing *Hes1* promoter was used as a reporter vector and RSV-renilla vector was used as a control vector. HeLa cells were transiently transfected with these reporters and each Ikaros or/and Helios expression vector by Lipofectamine 2000 reagent (Invitrogen). The luciferase activities were quantified by the Dual-Luciferase Reporter Assay System (Promega) at 24 h post-transfection.

**Retroviral construction and transduction.** The FLAG-Hel-5 cDNA sequence was subcloned into retrovirus vector pRxpuro. Stable cell populations expressing Hel-5 were selected by puromycin. The shRNA-expressing retroviral vectors and virus production procedures have been established.<sup>(3)</sup> The shRNA sequences are listed in Table S2. Stable cell populations were obtained by puromycin or G418 selection.

**Proliferation assays.** Cells ( $0.5$  or  $1.0 \times 10^4$ ) were plated in 96-well plates with media supplemented with 10% or 0.2% FCS. The cell numbers were evaluated for 4 days by Cell Counting Kit-8 (Dojindo, Kumamoto, Japan). The averages of at least three independent experiments are shown.

**Gene expression microarray analyses.** Gene expression microarray used the  $4 \times 44K$  Whole Human Genome Oligo Microarray (Agilent Technologies, Santa Clara, CA, USA); detailed methods were previously reported.<sup>(3)</sup> Coordinates have been deposited in the Gene Expression Omnibus database with accession numbers GSE33615 (gene expression microarray), GSE33602 (copy number analyses), and GSE41796 (Jurkat models).

## Results

**Abnormal expression of short Helios transcripts in primary ATL cells.** To characterize the gene expression signature in primary ATL cells, we previously carried out mRNA microarray analyses on a large number of samples. The comprehensive survey unveiled deregulated expression of Ikaros family genes; transcription levels of Ikaros and Aiolos were downregulated in ATL samples, whereas Helios was upregulated (Fig. S1). Thus,

we examined the detailed expression patterns and levels of Ikaros family members in PBMCs derived from a panel of ATL patients and HTLV-1 carriers (Fig. 1a). Compared with control PBMCs from normal volunteers (Fig. 1b), the expression levels of Ikaros and Aiolos seemed to be downregulated in ATL samples, consistent with our microarray results. However, there were obvious abnormalities in the expression patterns of Helios. The main isoform of Helios was changed from full-length Hel-1 to Hel-2, which lacks exon 3 that contains the first N-terminal zinc finger in the DNA-binding domain. In addition, four ATL-specific Helios short transcripts were identified (Fig. 1c). Among them, Hel-5 and Hel-6 have been reported to be expressed in ATL.<sup>29</sup> We also identified two novel variants, Hel-v1 that lacks exons 3 and 4 and Hel-v2 that lacks exons 2, 3, and 6. These abnormal Helios variants were also expressed in the samples of high-risk HTLV-1 carriers, who subsequently developed ATL in the next few years. Furthermore, nested PCR revealed that Hel-5 or Hel-6 were expressed in a majority of ATL samples (17/22 acute cases, 10/10 chronic cases, and 5/5 smoldering cases; total, 32/37 cases) (Fig. 1d, upper panels), whereas Hel-v1 was expressed only in limited cases of ATL (Fig. 1d, lower panels). In four cases, Helios was not expressed. Collectively, our mRNA analysis showed that Helios expression was generally deregulated in ATL cells.

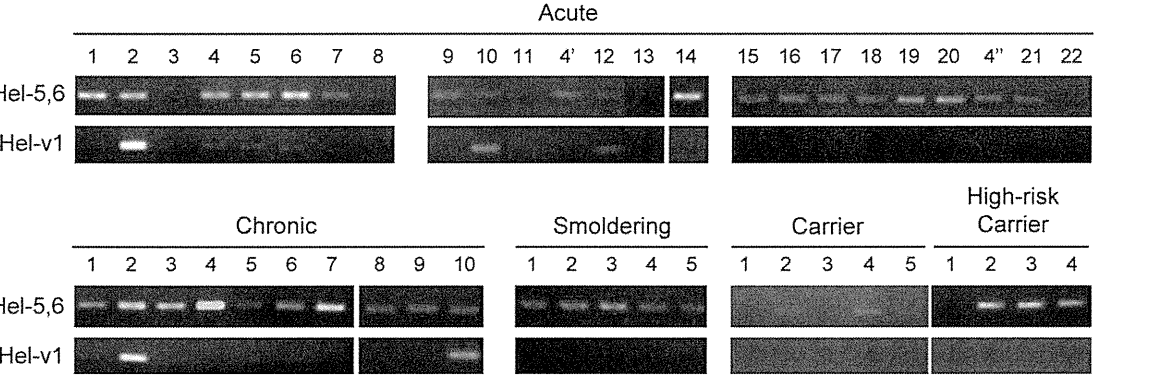
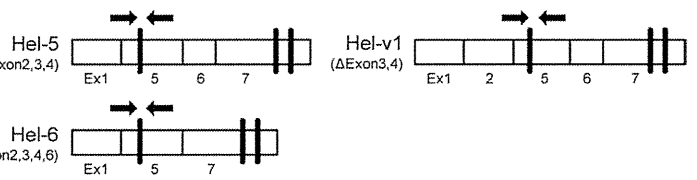
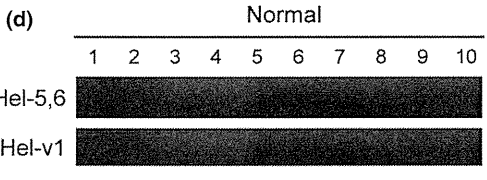
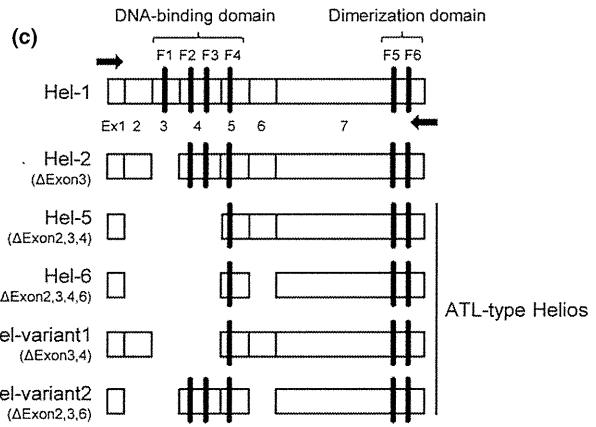
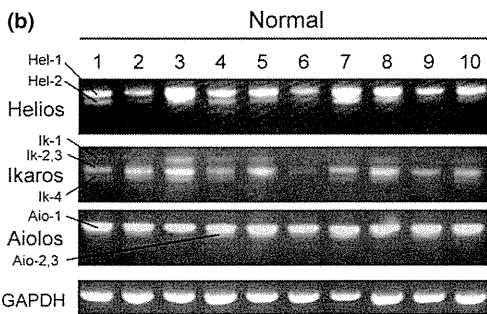
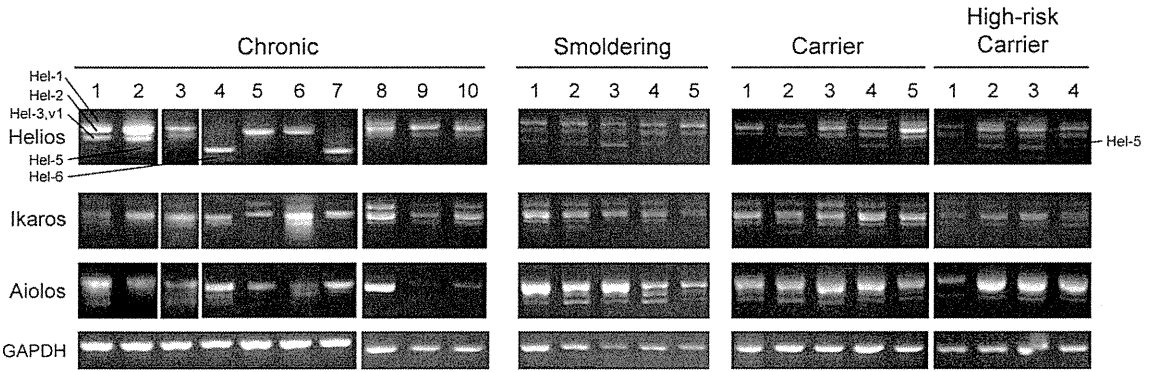
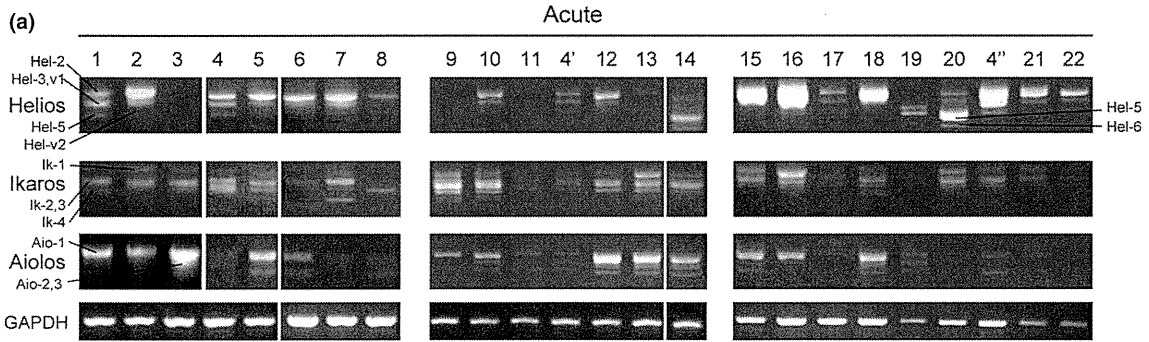
### Genomic abnormalities at the *Helios* locus in primary ATL cells.

To investigate the *Helios* locus in ATL, we retrieved data from our gene copy number analysis<sup>(3)</sup> and found that specific genomic deletion was accumulated at the *Helios* locus in ATL samples (17/168 cases, Fig. 2). All 17 cases were aggressive-type ATL (12/17 lymphoma types and 5/17 acute types). Furthermore, we found that two acute ATL cases in Figure 1(a) (#9 and #14), which showed severely deregulated or lost Helios expression, had a genomic deletion of the *Helios* locus.

**Dimerization ability of ATL-type Helios isoforms with wild-type Helios or Ikaros.** Consistent with a previously published report,<sup>(33)</sup> co-immunoprecipitation analyses confirmed that wild-type Hel-1 formed homodimers with themselves and heterodimers with wild-type Ikaros (Ik-1) protein (Fig. 3a, top panel, lane 1 and lane 4). In contrast, the dimerization activity of another artificial Helios mutant (Hel- $\Delta$ C), which lacks the dimerization domain at the C-terminal region, was dramatically declined (Fig. 3b, top panel, lane 1 and lane 4). We confirmed that all ATL-type Helios proteins could interact with Hel-1 and Ik-1, despite the fact that all of them lack various sets of the N-terminal exons (Fig. 3c–f).

**Cytoplasmic localization of ATL-type Helios isoforms lacking exon 6.** Ectopically expressed Hel-1 and Ik-1 were localized in the nucleus (Fig. 4a, top two panels). Regarding the ATL-type Helios isoforms, we found that Hel-5 and Hel-v1 were localized in the nucleus, whereas Hel-6 and Hel-v2, both of which lack exon 6, were substantially localized in the cytoplasm (Fig. 4a, middle four panels). We also confirmed the cytoplasmic localization of Hel- $\Delta$ exon 6, which is an artificial Helios mutant lacking only exon 6 (Fig. 4a, bottom panel). Thus, exon 6 appears to be critical for nuclear localization of Helios proteins. Furthermore, defect of exon 6 led to disruption of the

**Fig. 1.** (On the next page) Abnormal expression of Helios mRNA in primary adult T-cell leukemia (ATL) cells. (a) Expression analysis of Ikaros family genes in PBMCs by full-length RT-PCR (Acute,  $n = 22$ ; Chronic,  $n = 10$ ; Smoldering,  $n = 5$ ; HTLV-1 carriers,  $n = 5$ ; High-risk carriers,  $n = 4$ ). To detect and distinguish alternative splicing variants, PCR analyses were carried out with the sense and antisense primer sets designed in the first and final exons of each full-length transcript of Ikaros family genes. Obtained cDNAs were cloned and their sequences were analyzed. The samples acute #4, 4', and 4'' were derived from the same patient, but were studied independently. (b) Expression of Ikaros family genes in PBMCs from normal volunteers ( $n = 10$ ). (c) Schematic representation of Hel-1, Hel-2, and ATL-type Helios isoforms identified in this study. Hel-variant 1 (Hel-v1) and Hel-variant 2 (Hel-v2) are novel isoforms in ATL. Arrows indicate primer locations of full-length PCR for Helios. Ex, exon; F1–F6, functional zinc-finger domains. (d) Nested PCR with specific primer sets, which were designed at exon junction of exon 1–5 or exon 2–5 for detection of Hel-5 and Hel-6 (upper panel), or detection of Hel-v1 (lower panel), respectively. Arrows indicate primer locations.





cellular localization of binding partners. When Hel-6 or Hel-v2 were co-expressed with Hel-1 or Ik-1, they were co-localized in the cytoplasm (Fig. 4b, Fig. S2).

**Dominant-negative function of ATL-type Helios isoforms against wild-type Helios and Ikaros.** We next examined the

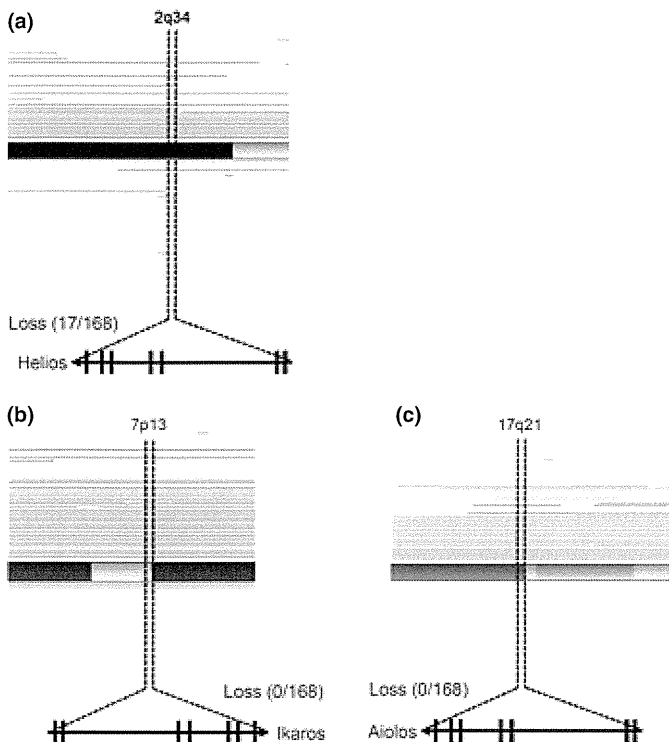


**Fig. 2.** Genetic abnormalities in *Helios* locus in primary adult T-cell leukemia cells. The results of our copy number analyses<sup>(3)</sup> (total number,  $n = 168$ ; acute type,  $n = 35$ ; chronic type,  $n = 41$ ; lymphoma type,  $n = 44$ ; smoldering type,  $n = 10$ ; intermediate,  $n = 1$ ; unknown diagnosis,  $n = 37$ ). Tumor-associated deletion of *Helios* region (17/168) was detected (a). No specific genomic losses were observed in *Ikaros* (b) or *Aiolos* loci (c). Recurrent genetic changes are depicted by horizontal lines based on Copy Number Analyser for GeneChip output of the single nucleotide polymorphism array analysis.

functional aspects of these ATL-type Helios isoforms by evaluating their DNA-binding capacities. For EMSA, we used an oligonucleotide probe derived from the promoter region of human *Hes1*, which was a direct target of Ikaros.<sup>(34,35)</sup> Ectopically expressed Hel-1 or Ik-1 could bind human *Hes1* promoter DNA (Fig. 5a). Supershift assays confirmed the binding specificity (Fig. 5b). In contrast, all ATL-type Helios isoforms did not show any specific binding to the *Hes1* promoter (Fig. 5a). This impossibility of specific DNA binding of ATL-type Helios was confirmed with another independent DNA probe, IkBS4<sup>(33,36)</sup> (data not shown). In addition, it was found in co-expression experiments that Hel-5 had antagonistic effects on the DNA binding capacity of Ik-1 in a dose-dependent manner (Fig. 5c). Reporter assays showed that Hel-1 and Ik-1 suppressed *Hes1* promoter activity. However, ATL-type Helios isoforms did not show any suppressive activity, and actually slightly activated the promoter (Fig. 5d). Furthermore, they also inhibited the suppressive function of Hel-1 and Ik-1 in a dose-dependent manner (Fig. 5e, Fig. S3). These data clearly indicate that ATL-type Helios isoforms are functionally defective because of a DNA binding deficiency and act dominant-negatively in transcriptional suppression induced by Hel-1 or Ik-1. We also confirmed that Hel-2, which lacks only exon 3 and is a major isoform in ATL cells, did not possess suppressive activity against *Hes1* promoter in spite of having binding activity (Fig. 5a,d).

**Major ATL-type Helios variant, Hel-5, promotes T cell growth.** Given the tumor-suppressive roles of Ikaros family members,<sup>(12-15)</sup> it was expected that abnormal splicing of Helios could contribute to T cell leukemogenesis. The mRNA level of Helios was significantly downregulated in ATL-related cell lines compared with that in T-cell lines without HTLV-1 (Fig. 6a, Fig. S4). Moreover, Helios protein was not detected in any ATL-derived or HTLV-1-infected cell lines used in this study (Fig. 6b). In contrast, the expression levels of Ikaros mRNA did not show major differences between HTLV-1-infected and uninfected T-cell lines. Those of Aiolos were low in most cell lines irrespective of HTLV-1 infection (Fig. 6a, Fig. S4). Ikaros protein was detected in all T-cell lines used in this study (Fig. 6b). To elucidate the cellular effects of the expression of dominant-negative ATL-type Helios isoforms in T cells, we established stable Jurkat cells expressing Hel-5 (Fig. 6c). A cell proliferation assay confirmed that Hel-5 expression significantly promoted Jurkat cell proliferation

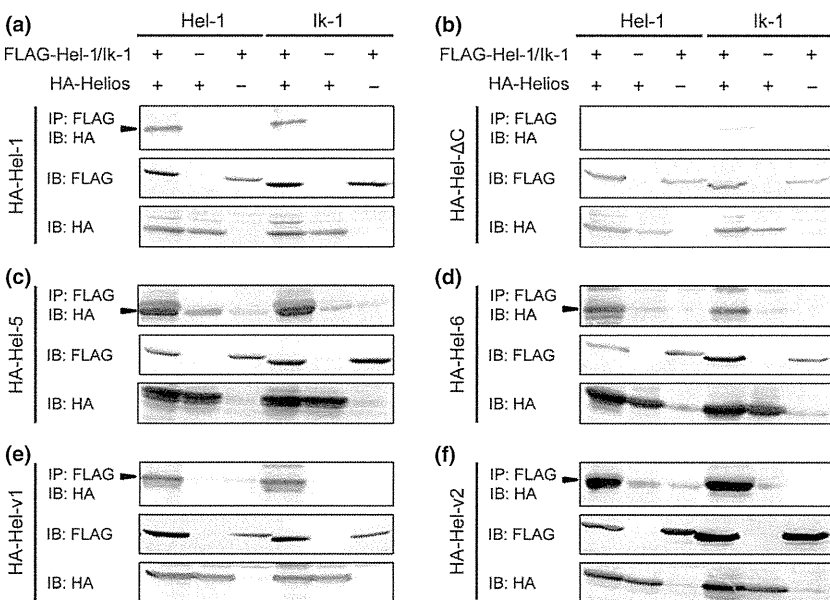


**Fig. 3.** Dimerization ability of adult T-cell leukemia (ATL-type) Helios isoforms. *In vitro* dimerization assays by co-immunoprecipitation between ATL-type Helios and wild-type Helios or Ikaros proteins. 293T cells were transfected with the indicated combination of expression vectors and subjected to co-immunoprecipitation analyses (top panels). Arrowheads indicate the complex of FLAG and HA-tagged proteins. Middle and bottom panels show the input samples. Hel-1 (a) and Hel- $\Delta$ C (b) included as positive and negative controls, respectively. ATL-specific isoforms, Hel-5 (c), Hel-6 (d), Hel-v1 (e), and Hel-v2 (f) were tested. IB, immunoblot; IP, immunoprecipitant.

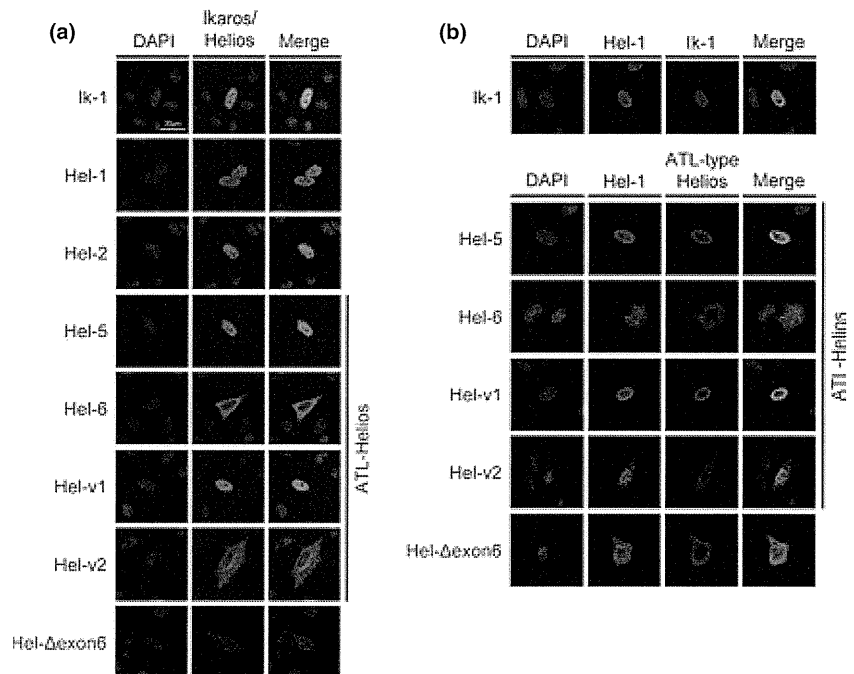


**Fig. 4.** Subcellular localization of adult T-cell leukemia (ATL)-type Helios isoforms. Immunostaining analyses of Helios and Ikaros proteins. HeLa cells were transfected with each individual expression vector (a) or the indicated combination of expression vectors (b). Each protein was visualized with anti-FLAG (green) or anti-HA antibodies (red). Nuclei were detected by DAPI staining (blue). Colocalization between Ik-1 and ATL-type Helios was shown in Fig. S2. Hel-v1, Hel-variant 1; Hel-v2, Hel-variant 2.

(Fig. 6d). To examine whether the cellular effect of Hel-5 was due to its dominant-negative function against Hel-1 and Ik-1, we carried out further knockdown analyses with specific shRNAs (Fig. 6e). The results showed that knockdown of wild-type Helios or Ikaros led to enhanced cell growth (Fig. 6f), which was consistent with the results of enforced Hel-5 expression. These results collectively suggested that counteraction of Ikaros or Helios by dominant-negative isoforms contributed to T cell growth.

**Helios deficiency causes expression of various genes in T cells.** We globally searched mRNA expression changes using microarray analysis of Jurkat cells expressing Hel-5 and those of knocked-down Helios or Ikaros (Fig. 7a,b). The results clearly showed differentially expressed gene sets between the transformants and control cells (Fig. 7c). Furthermore, pathway analysis<sup>(37)</sup> of each upregulated gene set identified activation of several signaling cascades. In particular, we focused on six common pathways identified in both Hel-5 transduced and Helios or Ikaros knocked-down Jurkat cells (Fig. 7d). These pathways are important for various T cell regulations, for example, cell growth, apoptosis resistance, and migration activity. Among these pathways, it has not been reported that the shingosine-1-phosphate (S1P) pathway is regulated by the Ikaros family. We confirmed overexpressed *S1PR1* and *S1PR3*, which are critical receptors for the activation of the S1P pathway, in manipulated Jurkat samples (Fig. 7e).

## Discussion

In the present study, on the basis of the integrated analysis of ATL cells using our biomaterial bank in Japan, we revealed a novel molecular characteristic of ATL cells, which is a profound abnormality in the expression of Helios. The abnormal alternative splicing and, in some cases, loss of Helios expression appear to be a part of the basis for advantageous cell growth and survival in ATL cells. We also showed the tumor-suppressive function and target genes, as well as pathways of Helios, in mature human T cells.

Characterization of Ikaros family members revealed profound abnormalities in Helios expression in ATL cells: (i)

biased and increased expression of alternatively spliced variants; (ii) suppression of Hel-1 expression; (iii) lack of Helios expression in some cases; and (iv) frequent genomic defects of the *Helios* locus. Our results also revealed that alternatively spliced Helios variants are expressed in PBMCs of HTLV-1 carriers, suggesting that the abnormal splicing of Helios may occur in HTLV-1-infected cells at the carrier state until progression to leukemia development. However, the genomic deletions appear to be one of the important genetic events during the latter stages of leukemia development, as they were observed only in aggressive subtypes of ATL.

The structural characteristics of the ATL-type Helios variants involve a selective lack of one or more zinc fingers in the N-terminal domain. The results of this study indicated that these variant proteins lost DNA binding activity, whereas the capacity of dimerization was preserved. Therefore, these variant proteins hindered transcriptional activities of Ikaros family proteins, showing dominant-negative effects. In addition, a part of ATL-type Helios isoform, which lacks exon 6, is linked to abnormal localization of wild-type Helios and Ikaros. We confirmed that Helios isoforms lacking exon 6 were overexpressed in primary ATL cells (Fig. S5). Interestingly, Hel-2 has reduced transcriptional suppressive activity compared with Hel-1, although it can bind to the target sequence as well as Hel-1. This is similar to a previous report,<sup>(36)</sup> which noted that the activity of mouse Ik-2 protein for the reporter gene was remarkably lower than that of Ik-1, whereas the binding affinities of Ik-1 and Ik-2 were similar. The exon 3 skip occurred more frequently in ATL cells, compared to PBMCs from normal volunteers (Fig. S6). These results collectively indicate that all abnormalities of Helios expression, including loss of or decreased Hel-1 expression and upregulated Hel-2 and ATL-type Helios, result in abrogation of Ikaros family functions in ATL cells.

We also confirmed that *Hes1*, a target gene of the Notch pathway, is one of the targets of Helios as well as Ikaros.<sup>(34,35)</sup> A recent study reported that activated Notch signaling may be important to ATL pathogenesis and that *Hes1* is upregulated in ATL cells.<sup>(38)</sup> Thus, we examined expression levels of *Hes1* mRNA by quantitative RT-PCR and confirmed the

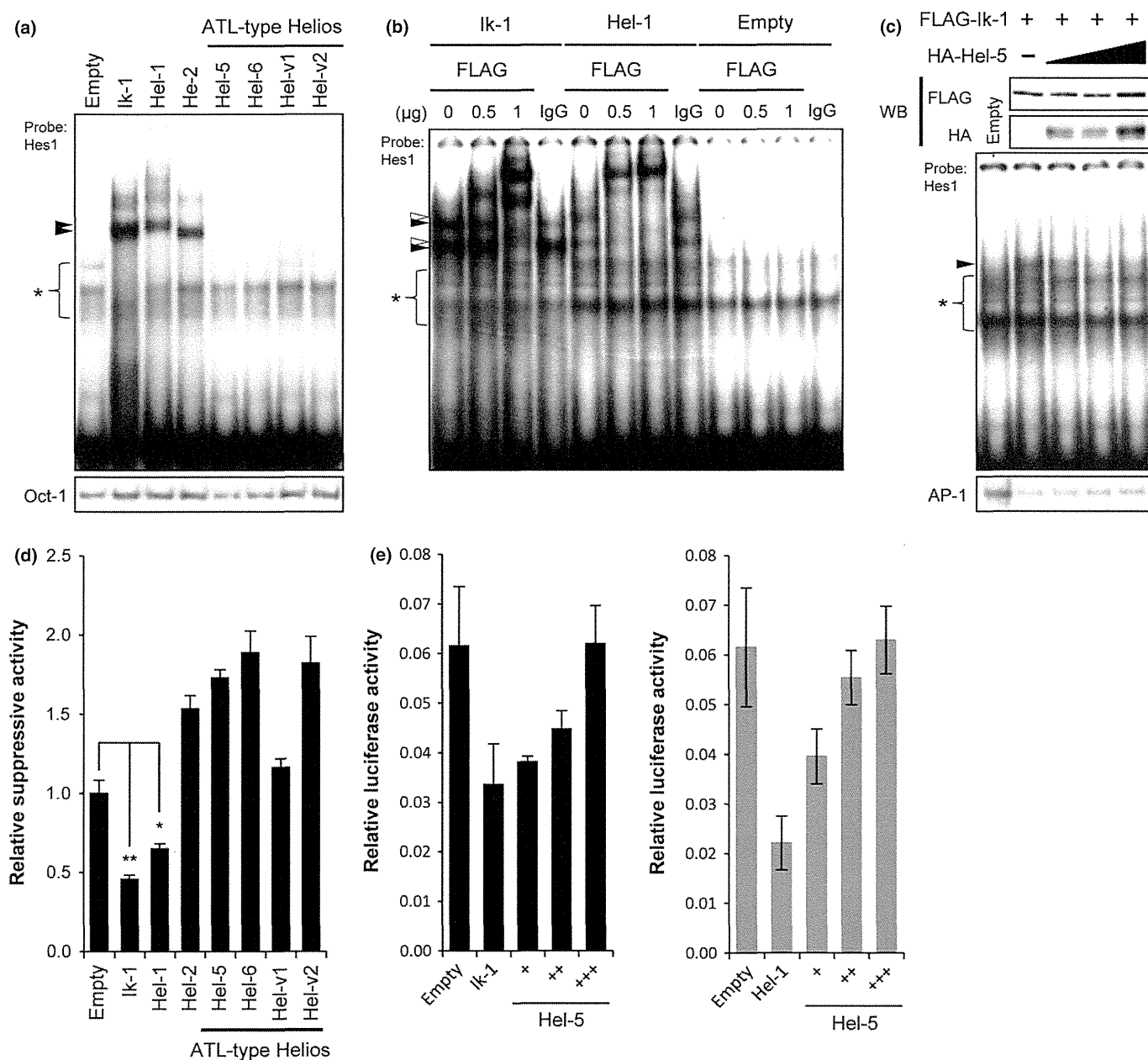


**Fig. 5.** Dominant-negative function of adult T-cell leukemia (ATL)-type Helios isoforms. (a) DNA-binding activities of wild-type Helios or Ikaros and ATL-type Helios proteins. Each FLAG-tagged Helios or Ikaros isoforms were ectopically expressed in 293T cells and their nuclear extracts were subjected to EMSA with a [ $\gamma$ - $^{32}$ P]-labeled *Hes1* promoter probe. Oct-1 probe was used as an internal control. Arrowheads indicate Helios or Ikaros complexes. \*Non-specific bands. Hel-v1, Hel-variant 1; Hel-v2, Hel-variant 2. (b) Results of supershift assays. Anti-FLAG (0, 0.5, 1  $\mu$ g) or control IgG (1  $\mu$ g) antibodies were added to each nuclear extract prior to electrophoresis. The black and white arrowheads indicate the supershifted bands of Ik-1 and Hel-1, respectively. (c) Antagonistic effects of Hel-5 on DNA-binding of Ik-1 tested by EMSA. The molar ratios of Ik-1 to Hel-5 plasmids are 1:1, 1:4, and 1:8. Expression levels of FLAG-Ik-1 and HA-Hel-5 were assessed by immunoblotting. The arrowheads indicate the Ik-1 specific band. AP-1 probe was used as an internal control. WB, western blot. (d) Transcriptional suppression activities of various Helios or Ikaros isoforms tested by *Hes1* promoter-luciferase reporter systems ( $n = 3$ , mean  $\pm$  SD). Basal *Hes1* promoter activity was defined as firefly/renilla ratio, and suppression activities of Helios or Ikaros are relatively presented. Statistical significance was evaluated by unpaired Student's *t*-test (\* $P < 0.05$ ; \*\* $P < 0.01$ ). (e) Inhibitory function of Hel-5 against Ik-1 and Hel-1 tested by *Hes1* promoter assay ( $n = 3$ , mean  $\pm$  SD). The molar ratios of Ik-1 or Hel-1 to Hel-5 plasmids are 1:1, 1:2, and 1:3. Relative luciferase activities were defined as firefly/renilla ratio.

upregulation in our ATL samples (Fig. S7). *Hes1* has been reported to directly promote cell proliferation through the transcriptional repression of p27kip1.<sup>(39)</sup> Taken together, our results suggest a possibility that abnormalities in Helios expression are one of the causes of *Hes1* activation, which may be one of the genetic events involved in ATL leukemogenesis.

Our results show that the Hel-5 variant may have an oncogenic role, whereas the wild-type Helios, Hel-1, shows

tumor suppressor-like activity. These findings are consistent with previous findings in mice.<sup>(15)</sup> Furthermore, our description of expression profiles of stable cells followed by pathway analyses showed activation of several important pathways in lymphocytes for the regulation of proliferation, survival, and others. In particular, we discovered novel molecular cross-talk between the Ikaros family and the S1P pathway. The S1P-S1PR1 axis is known to play important

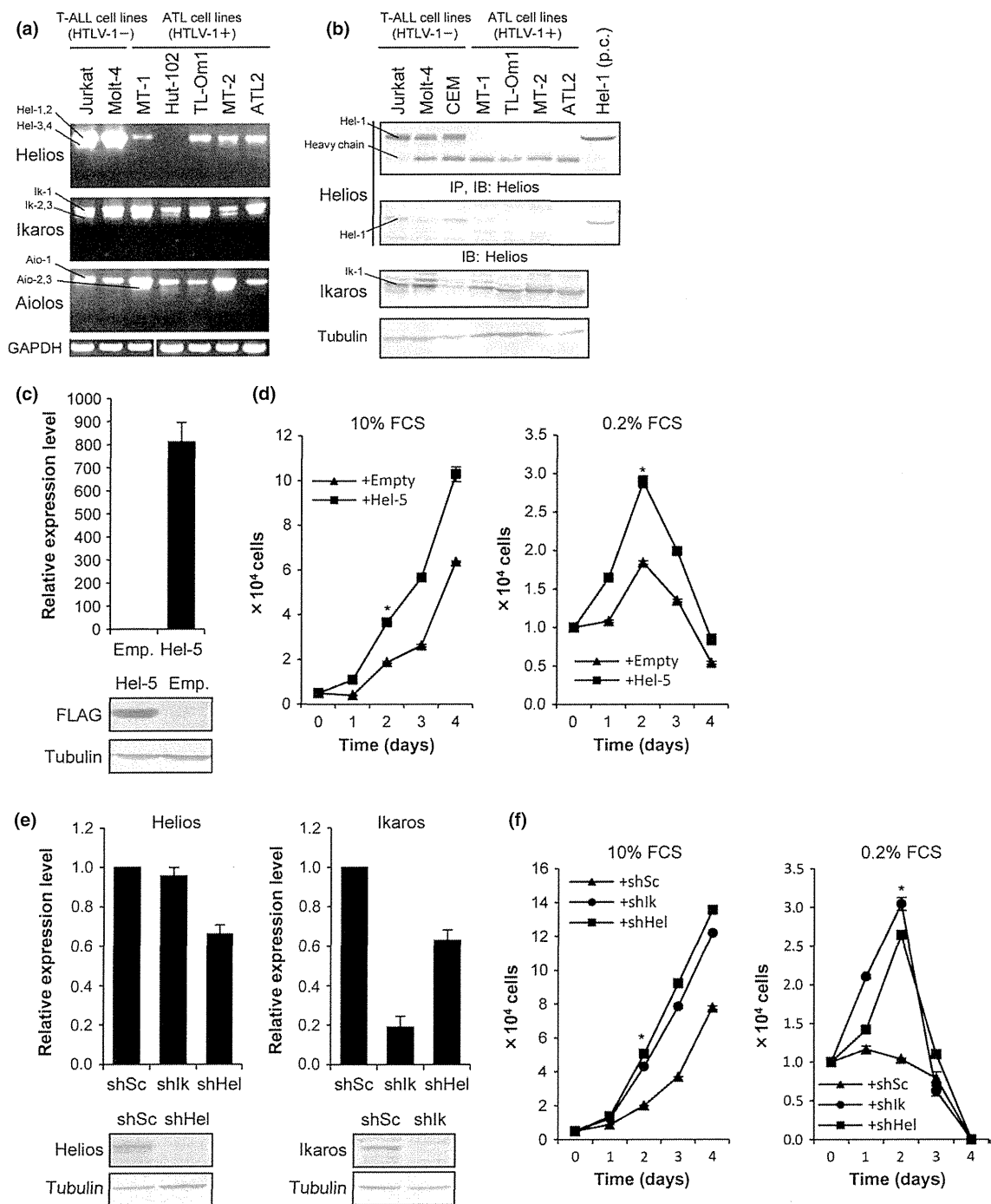


**Fig. 6.** Hel-5 functions in T cell growth and survival. (a) Expression patterns and levels of Ikaros family genes in various cell lines examined by RT-PCR. ATL, adult T-cell leukemia; T-ALL, acute T lymphoblastic leukemia. (b) Results of immunoblotting analyses of the immunoprecipitants (top panel) and cell lysates (lower panels). Positive control (p.c.), Hel-1 transfectant. IB, immunoblot; IP, immunoprecipitant. (c) Establishment of Jurkat cells stably expressing Hel-5. The Hel-5 level was quantified by quantitative RT-PCR (top,  $n = 3$ , mean  $\pm$  SD) and immunoblotting (bottom). (d) Cell proliferation analysis of control cells (▲) and Hel-5-expressing Jurkat cells (■) under two FCS conditions ( $n = 3$ , mean  $\pm$  SD). Statistical significance was observed ( $*P < 0.01$ , Student's  $t$ -test). (e) Knockdown analyses of Helios or Ikaros in Jurkat cells. The Helios and Ikaros levels were evaluated by quantitative RT-PCR (top,  $n = 3$ , mean  $\pm$  SD) and immunoblotting (bottom), respectively. (f) Cell proliferation curves of scrambled shRNA (shSc) cells (▲), shIkaros (shIk) cells (●), and shHelios (shHel) cells (■) were examined in two FBS conditions ( $n = 3$ , mean  $\pm$  SD;  $*P < 0.01$ ).

roles in regulation of the immune system, apoptosis, cell cycle, and migration of lymphocytes.<sup>(40-42)</sup> Recently, activation of the S1P pathway in various diseases, including leukemia, has been reported, and the therapeutic potential of S1PR1 inhibitors was suggested.<sup>(42)</sup> Studies of functional roles of S1P pathway activation in ATL cells are now underway in our laboratory.

In conclusion, our present study revealed a novel aspect of molecular abnormalities in ATL cells: a profound deregulation in Helios expression, which appears to play an important role in T-cell proliferation. Our experimental approaches also imply that, in addition to genetic and epigenetic abnormalities, ATL shows abnormal splicing, which has been observed in various human diseases including cancers.<sup>(43-45)</sup>